J. Membrane Biol. 36, 337–372 (1977)

Passive Ionic Properties of Frog Retinal Pigment Epithelium

Sheldon S. Miller* and Roy H. Steinberg

Department of Physiology, University of California, San Francisco, California 94143

Received 12 May 1976; revised 24 January 1977

Summary. The isolated pigment epithelium and choroid of frog was mounted in a chamber so that the apical surfaces of the epithelial cells and the choroid were exposed to separate solutions. The apical membrane of these cells was penetrated with microelectrodes and the mean apical membrane potential was −88 mV. The basal membrane potential was depolarized by the amount of the transepithelial potential (8–20 mV). Changes in apical and basal cell membrane voltage were produced by changing ion concentrations on one or both sides of the tissue. Although these voltage changes were altered by shunting and changes in membrane resistance, it was possible to estimate apical and basal cell membrane and shunt resistance, and the relative ionic conductance T_i of each membrane. For the apical membrane: $T_K \cong 0.52$, $T_{HCO_3} \cong 0.39$ and $T_{Na} \cong 0.05$, and its specific resistance was estimated to be 6000–7000 Ω cm^2. For the basal membrane: $T_K \cong 0.90$ and its specific resistance was estimated to be 400–1200 Ω cm^2. From the basal potassium voltage responses the intracellular potassium concentration was estimated at 110 mM. The shunt resistance consisted of two pathways: a paracellular one, due to the junctional complexes and another, around the edge of the tissue, due to the imperfect nature of the mechanical seal. In well-sealed tissues, the specific resistance of the shunt was about ten times the apical plus basal membrane specific resistances. This epithelium, therefore, should be considered "tight". The shunt pathway did not distinguish between anions (HCO_3^-, Cl^-, methylsulfate, isethionate) but did distinguish between Na^+ and K^+.

The pigment epithelial cells and the photoreceptors are closely associated in the vertebrate retina. Apical processes from the pigment epithelial cells lie alongside and, in some cases, surround the photoreceptor outer segments. The epithelium also separates the sensory retina from its choroidal blood supply and transports salts and metabolites to and from the retina (Dowling, 1960; Noell, Crapper & Paganelli, 1965; Lasansky & DeFisch, 1966; Young, 1969). Our approach to questions of

**Present address and correspondence:* School of Optometry, 101 Minor Hall, University of California, Berkeley, California 94720.

pigment epithelial transport and ionic interactions with photoreceptors is first to describe the ionic properties of the apical and basal membranes of the epithelium. Two kinds of experiments were undertaken: ion flux measurements (Miller & Steinberg, 1977) and, as reported here, the recording of intracellular voltage responses to changes in ion concentrations.

In these experiments, the isolated pigment epithelium-choroid was mounted so that the apical and choroidal surfaces of the pigment epithelium could separately be exposed to different solutions. The purpose was to quantify the passive ionic properties of the apical and basal cell membranes. Electrical shunting across the preparation, however, complicated the analysis of the membrane voltage responses, by reducing their magnitude (Boulpaep, 1967, 1971; Rose & Schultz, 1971; Schultz, 1974). An analysis was developed that allowed us to correct for these reductions and, therefore, to calculate the resistances and relative ionic conductances of each cell membrane.

Materials and Methods

Anatomy

Three tissues form the posterior portion of the eyeball (Fig. 1*A*). Two originate from mesoderm—the sclera, an outermost collagenous layer, and the choroid, a middle vascular layer. The innermost layer, the retina, originates from neuroectoderm and consists of a layer of epithelial cells—the pigment epithelium, and the sensory retina. In the frog, individual pigment epithelial cells measure about 15 μm both in width and depth (Porter & Yamada, 1960; Nilsson, 1964; Steinberg, 1973). The junctional complexes connecting these cells in frogs differ from those of other species by being absent at the cellular apices; they begin about halfway down the lateral surfaces of each cell (Porter & Yamada, 1960; Hudspeth & Yee, 1973). Gap junctions occur most apically, Z. adherens most basally and Z. occludentes (tight junctions) also are unusual because they overlap the gap junctions and Z. adherens, although they still form a broad, continuous band around each cell (Hudspeth & Yee, 1973). The apical surfaces of the cells face the sensory retina and are covered with villouslike processes that are closely apposed to the photoreceptors (Fig. 1*B*, *C*). These processes are very long, extending down to the photoreceptor inner segments, a total distance of 60–95 μm (Nilsson, 1964). The epithelial cells' basal surfaces face the choroidal blood supply, and the plasma membrane of the basal surface tends to infold repeatedly although these infoldings are not prominent in frogs (Kuwabara, *in press*).

A layer of collagen fibrils and elastic fibers, Bruch's membrane, firmly attaches the basal surface of the epithelial layer to the choroid, and so these tissues cannot be readily separated from each other. The choroid consists, for the most part, of blood vessels and melanocytes dispersed in a fibrous stroma; and directly beneath Bruch's membrane, it forms a dense bed of thin-walled, wide-lumened, fenestrated capillaries. Larger blood vessels occur further out in the choroid and these branch from vessels that penetrate the eyeball through the sclera. At those points the sclera firmly adheres to the choroid; but in intervening areas the choroid and sclera are attached by only a thin layer of collagen fibrils that can be easily dissected away.

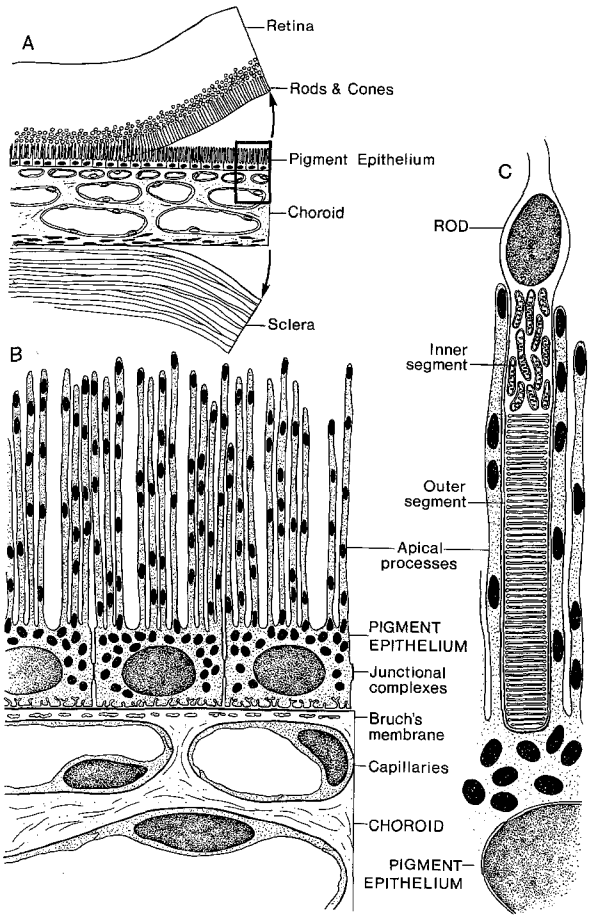

Fig. 1. Diagram of the tissue. (*A*) Removal of sensory retina and sclera from pigment epithelium-choroid. (*B*) Detail of pigment epithelium-choroid. (*C*) Detail of association between pigment epithelial apical processes and red rods (after Nilsson, 1964)

Mounting

Large bullfrogs, *Rana catesbiana*, were obtained from Californian and Midwestern suppliers, and kept from several days to several weeks in running tap water at 17.5 °C, on an alternating 12-hr cycle of light and darkness. Well dark-adapted frogs were decapitated, the eye enucleated and then sectioned behind the lens into anterior and posterior portions. The posterior portion, consisting of retina, choroid and sclera was sectioned through the optic disc into two pieces. Each piece was then trimmed to a square of about 6.5 mm, taking care to remove all areas of Ora Serrata, since the epithelium and retina are firmly attached there. After placing the pieces in solution, the sensory retina was peeled away from the pigment epithelium, and the sclera dissected from the choroid (Fig. 1*A*). The remaining tissue, consisting of pigment epithelium and choroid (Fig. 1*B*), was then mounted in a chamber (Fig. 2).

The method of mounting the tissue was copied from the one originally described for the toad (Lasansky & DeFisch, 1966). We had tried a large number of other methods, all

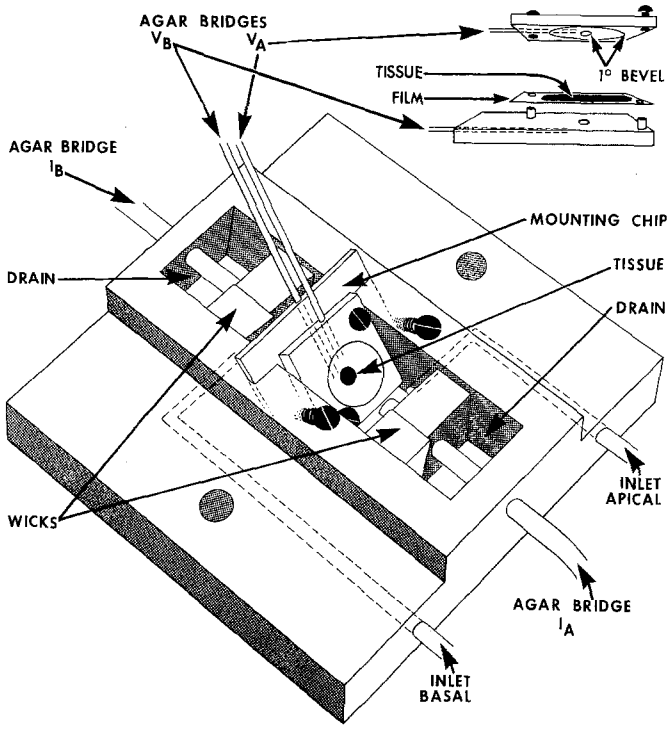

Fig. 2. Diagram of the experimental chamber. The insert shows the three parts of the mounting chip: top and bottom plates, and X-ray film

unsuccessfully, including use of tissue adhesives such as isobutyl-2-cyanacrylate (Helman & Miller, 1973). The mounting chip consisted of bottom and top lucite plates and an interposed piece of X-ray film, all having 3 mm centered circular holes 0.07 cm^2 area (Fig. 2, inset). The surface of the top plate that faced the tissue has a 1° bevel extending 10 mm from the center of the hole. This created a space between the film and top plate that diminished in height gradually from the edge of the 3 mm hole, where it was 90 μm, out to 10 mm. When the top plate was attached to the bottom plate, therefore, compression of the tissue increased with distance from the edge of the hole. The surfaces of the film and lucite, which were to contact the tissue, were lightly coated with bovine albumin. While still submerged in solution the tissue was grasped gently on an edge, slid onto the film choroidal side down, and centered over the hole. The film was then pressed onto the plate, the facing surface of the film and plate having been lightly coated with a high vacuum silicone lubricant. Unnecessary damage to the edges of the tissue was avoided by finding the loosest attachment between top and bottom plates which would still seal the tissue. This was accomplished by screwing the plates together very slowly while observing the tissue with a dissecting microscope. The chip was coated on all edges with silicone lubricant and placed in the slot of the chamber at a 45° angle to facilitate microelectrode penetrations of the apical surface (Fig. 2).

Perfusion

The two sides of the tissue, *apical* surface of pigment epithelium *vs.* choroid, hereafter called *basal* surface, were immersed in 3.3 ml baths. The baths were continuously perfused

by gravity feed from large reservoirs and the solutions entering each chamber were switched by means of three-way Iso-latch valves (General Valve). The rate of flow into each chamber was adjusted by means of micrometer capillary valves (Gilmont) that were calibrated before each series of experiments. Fluid turbulence was minimized by having the solutions enter each bath through a small hole at the bottom and exit at the top through a filter paper wick into a small reservoir that was first emptied by suction. Later on, turbulence due to the suction was eliminated by using gravity to empty the small reservoirs into much larger reservoirs.

Response Time

Response latencies and times to maximum response were a function of flow rate and the size of the unstirred layer. We chose the fastest rates that would cause diffusion potentials to evolve rapidly without interfering with microelectrode stability, 8–12 cc/min. The response latency on the apical side, measured from the moment of switching, averaged 30 sec. Because the choroid acts as a large unstirred layer basal latencies were longer, usually 60 sec total. On either side, responses to 10-fold changes in concentration were *at least* 90% complete within 3 min from the start of the change and so they were measured at 3 min. In experiments where the solutions on both sides were changed together, the apical change was delayed by the latency difference between the two sides for that tissue. This assured that the apical and basal membranes would be exposed to the new solutions at the same time.

Recording

Electrodes. Two pairs of Agar-Ringer's bridges symmetrically placed on each side of the tissue (Figs. 2, 3; V_A, V_B, I_A, I_B) were used to record the transepithelial potential and to pass current through the tissue. Pigment epithelial cell membrane potentials were recorded with glass micropipettes filled by the fiberglass technique with either 3 M KCl or 5 M K Citrate. They were made from borosilicate glass, either 0.8 mm or 1.0 mm OD, and pulled on either a Livingston-type puller or an Industrial Science Associates puller. In some experiments they were bevelled by the technique of Brown and Flaming (1974). Resistances were from 25 to 100 MΩ. The micropipette was mounted on a hydraulic microdrive (David Kopf) that was itself held by a micromanipulator (Leitz).

Electrical circuit. Fig. 3 diagrams the electrical circuit that recorded the transepithelial potential (p.d.), passed current through the tissue, and recorded cell membrane potentials. The p.d. was recorded by means of two high impedance differential amplifiers, A_1 and A_2. The voltmeter V_2 indicated the true p.d. to within 0.1 mV. The voltmeter V_1 and one channel of the Brush recorder (PR_1) indicated the p.d. after a bucking voltage had been added or subtracted in order to compensate for a ± 0.5 mV electrode asymmetry potential.

For measurement of *IR* drops across the tissue or across either cell membrane, currents of up to 80 μA were supplied by a constant current source (*C*) that was turned on and off, either manually, or by a square-wave generator and stimulus isolation unit (Grass S-4). Current through the tissue was monitored on a meter (*I*), and on the Brush recorder (PR_1). *IR* drops between V_A and V_B for different solutions were measured in the absence of the tissue, and were automatically compensated by a circuit similar to the one of Rothe, Quay and Armstrong (1969).

To record the apical and basal cell membrane potentials, the micropipette was positioned intracellularly and referred to either V_A or V_B. The output of the micropipette

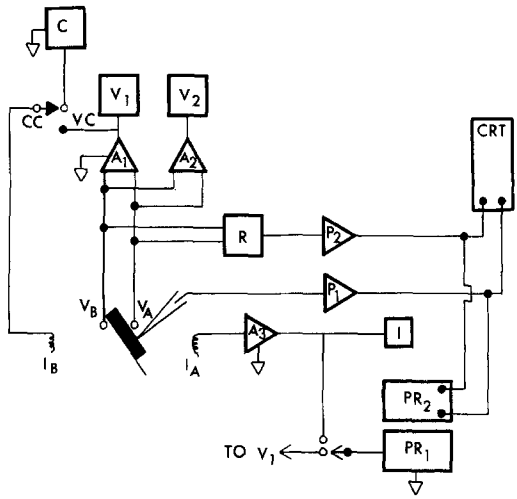

Fig. 3. Diagram of recording system. V_A, V_B, apical and basal voltage recording electrodes. I_A, I_B, apical and basal current passing electrodes. VC-CC, a switch used to pass current across the tissue, either from a constant current source (C) or from a voltage clamp (VC). The true transepithelial potential was indicated on voltmeter V_2, while V_1 also indicated this voltage, and a bucking voltage. When voltage clamping, V_1 indicated the error voltage of the clamp. Current passed through the tissue was monitored by means of a current to voltage converter (A_3) and meter (I). Cell membrane potentials were recorded between the microelectrode and reference, V_A or V_B, using two microelectrode preamplifiers (P_1, P_2) and high speed reed relays (R) to switch the reference. Membrane potentials were displayed on the oscilloscope (CRT) and on one channel of the pen recorder (PR_2). Clamp current or transepithelial potential was displayed on the other channel (PR_1)

and V_A or V_B were connected to microelectrode preamplifiers (model 1090, Winston) and displayed differentially on both an oscilloscope (Tektronix 565) and a pen recorder (Model 220, Brush). High speed reed relays (R) were used to switch the reference to V_A or V_B. By switching the relays at 20 Hz with a square-wave generator (Grass S-4), the apical and basal cell membrane potentials were "simultaneously" recorded.

Solutions

The steady-state perfusing solution was a modified Ringer's having the following composition (in mM): 82.5 NaCl, 27.5 $NaHCO_3$, 2 KCl, 1 $MgCl_2 \cdot 6H_2O$, 1.8 $CaCl_2$, 10 glucose and gassed with 95% O_2/5% CO_2 to a pH of 7.4 ± 0.1. The final osmolarity was 227 mosm. The HCO_3^- concentration $[HCO_3^-]_o$ was varied either by replacing $NaHCO_3$ with NaCl on a millimolar basis, or by keeping $[Cl^-]_o$ constant and replacing $NaHCO_3$ with sodium isethionate ($NaHOCH_2CH_2SO_3$) or sodium methylsulfate ($NaCH_3SO_4$). When $[HCO_3^-]_o$ was raised or lowered the CO_2 concentration also was raised or lowered, unless otherwise indicated, by gassing just prior to use with different percentage CO_2's until the solution reached the desired pH. The zero $[HCO_3^-]_o$ solution was buffered with 2.125 mM $NaH_2PO_4 \cdot H_2O - 0.375$ mM Na_2HPO_4. Other ion substitutions were: KCl for NaCl to vary $[K^+]_o$; Tris [Tris(hydroxymethyl)aminomethane] and

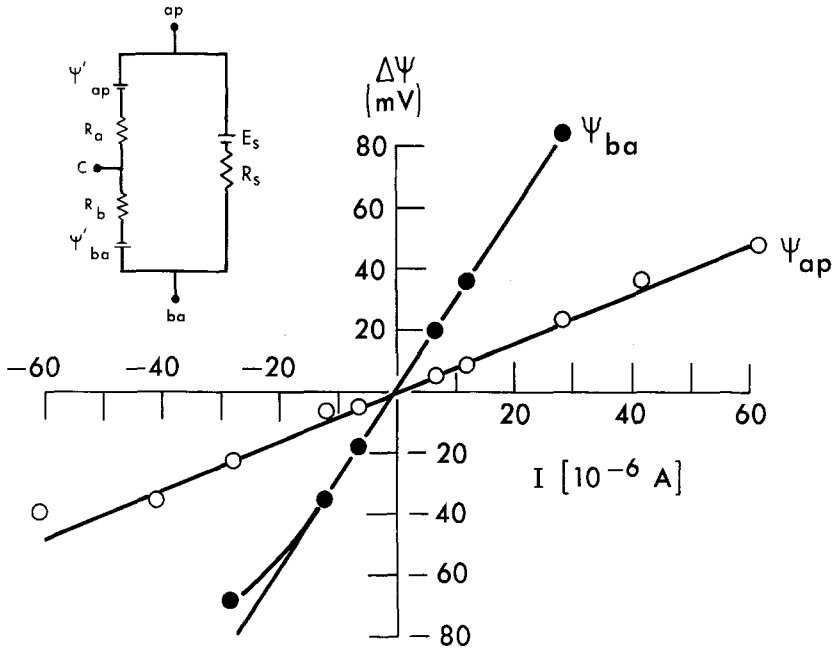

Fig. 4. Voltage deflections $\Delta\Psi_{ap}$ (○) and $\Delta\Psi_{ba}$ (●) as a function of transepithelial current. Positive current flows from basal to apical. All the voltage deflections were recorded across the membranes of one cell, from 0.25 to 0.50 sec after the onset of a 3.1 sec current pulse. Ψ_{ap} immediately after penetrating the cell was −90 mV. Insert: Electrical model of the pigment epithelium-choroid. The components of the model are defined in the text

choline HCO_3 for NaCl and $NaHCO_3$, to vary $[Na^+]_o$; and sodium isethionate or sodium methylsulfate for NaCl to vary $[Cl^-]_o$.

Liquid junction potentials that occurred when different solutions were placed in the two baths were calculated and some of the calculations verified by measurements in a model system (Barry & Diamond, 1970). Corrections were applied for liquid junction potentials in the $K^+ \rightleftarrows Na^+$ and $HCO_3^- \rightleftarrows Cl^-$ replacements. All results are given as mean ±SEM, unless otherwise indicated.

Theory

The object of this section is to present an electrical model for the epithelium (Fig. 4) and to derive equations that enable one to calculate the parameters of the model. The most important of these are the resistances and relative ionic conductances for each membrane. In this model, R_a is the resistance of the apical membrane, including the lateral cell membrane that lies apical to the junctional complex; and R_b is the resistance of the basal membrane, including the lateral cell membrane basal to the junctional complex and the choroid. The choroidal resistance is negligible relative to that of the basal membrane. This was confirmed by gently scraping the epithelium and observing that the remaining resistance approximates that of the solution between the external voltage electrodes. R_s is the total shunt resistance. It consists of paracellular, or junctional complex resistance, including the longitudinal resistance of the lateral intercellular

spaces; in parallel with an edge resistance, which *we assume must occur due to the method of mounting this tissue* (Helman & Miller, 1973). Evidence for this pathway comes from flux experiments (Miller & Steinberg, 1977) that show that the magnitudes of unidirectional transepithelial ion fluxes decrease as transepithelial resistance (R_t) increases, up to about 4000 Ω, and then remain constant up to the highest values of R_t (~9000 Ω).

Although the individual resistances cannot be directly measured, there are two resistance ratios that can be obtained by passing constant transepithelial current pulses across the tissue and monitoring the appropriate voltage response $\Delta\psi$. The ratios are defined as follows:

$$R_t = \frac{(R_a + R_b)R_s}{R_a + R_b + R_s} \quad \text{and} \quad a = \frac{\Delta\Psi_{ap}}{\Delta\Psi_{ba}} = \frac{R_a}{R_b}. \tag{1}$$

For a given pulse of current, R_t is determined from the change in transepithelial potential (TEP) and a from the ratio of apical to basal voltage drops (Frömter, 1972).

To determine the relative ionic conductances we have to know the relationship between the recorded apical and basal membrane potentials Ψ_{ap}, Ψ_{ba} and Ψ'_{ap}, Ψ'_{ba}, the potentials that would have been recorded if R_s were infinite. The relative ionic conductances can then be determined from the changes in Ψ'_{ap} and Ψ'_{ba}, $\Delta\Psi'_{ap}$ and $\Delta\Psi'_{ba}$, that are produced by changes in ion concentration. Since R_s is finite the microelectrode records $\Delta\Psi_{ap}$ and $\Delta\Psi_{ba}$, which are considerably smaller than $\Delta\Psi'_{ap}$ and $\Delta\Psi'_{ba}$, and so the relationship between these quantities must also be determined.

In the steady state, with identical solutions on both sides of the tissue, Ψ'_{ap} and Ψ'_{ba} are defined as follows:

$$\Psi'_{ap} = \frac{\sum_i g_{ai} E_i}{\sum_i g_{ai}}, \qquad \Psi'_{ba} = \frac{\sum_i g_{bi} E_i}{\sum_i g_{bi}} \tag{2}$$

where g_{ai}, g_{bi} refer to the apical and basal membrane conductances of the i^{th} ion and $\frac{1}{\sum g_{ai}} = R_a \left(\frac{1}{\sum g_{bi}} = R_b\right)$. These equalities follow from from the assumed mosaic nature of the membranes (Finkelstein & Mauro, 1963). E_i is the equilibrium potential for the i^{th} ion and

$$E_i = \frac{RT}{F} \ln \left[\frac{C_{\text{out}}}{C_{\text{in}}}\right]_i$$

where C_{out} and C_{in} represent the external and internal concentrations (the ratio of activity coefficients is taken to be one). Intracellular recordings show that the apical membrane potential Ψ_{ap} is more hyperpolarized than the basal membrane potential Ψ_{ba} by an amount equal to the transepithelial potential (TEP) which is 8–20 mV, apical side positive. Therefore, in the steady state, a current i flows around the loop, through R_s, polarizing the basal and apical membranes. The relationship between Ψ_{ap}, Ψ'_{ap} and Ψ_{ba}, Ψ'_{ba} is

$$\Psi_{ap} = \Psi'_{ap} - iR_a \tag{3a}$$

$$\Psi_{ba} = \Psi'_{ba} + iR_b \tag{3b}$$

where

$$i = \frac{\Psi'_{ap} - \Psi'_{ba} - E_s}{R_a + R_b + R_s}$$

and E_s is a battery that could arise when the tissue separates solutions of different ionic concentration. Some assumptions in this model are that the responses of all cells are identical and that under uniform stimulation no *net* current will flow between the cells.

This is supported by the finding, in other epithelia, including *Necturus* retinal pigment epithelium, that current injected intracellularly produces voltage responses across distant cell membranes that fall off radially with distance and are isotropic in the plane of the epithelial sheet (Frömter, 1972; Hudspeth & Yee, 1973; Reuss & Finn, 1974; Spenny, Shoemaker & Sachs, 1974; Spenny, Flemstrom, Shoemaker & Sachs, 1975).

Since the resistances may change during the solution composition changes, the analysis is divided into two cases. In the first case it is assumed after a solution composition change, that only Ψ_{ap}, Ψ_{ba} and TEP change, while a, R_s and R_t remain constant. The second case is the more general one where we assume that all of these resistances change.

Case I: a, R_t, R_s are Constant

In Eqs. (3a) and (3b) we let $a=\dfrac{R_a}{R_b}$ and eliminate i to obtain

$$\Psi_{ap}+a\Psi_{ba}=\Psi'_{ap}+a\Psi'_{ba}. \tag{4}$$

If, for example, we change the concentration of a permeant ion in the *basal* solution then

$$\Psi^*_{ap}+a\Psi^*_{ba}=\Psi'_{ap}+a\Psi'^*_{ba} \tag{5}$$

where the asteriks denote new potential values. Here, the change from $\Psi_{ap}\rightarrow\Psi^*_{ap}$ occurs because the basal membrane diffusion potential ($\Psi'_{ba}\rightarrow\Psi'^*_{ba}$) causes i to change. It is assumed that Ψ'_{ap} stays constant since only the basal bath was altered. Eq. (4) is subtracted from Eq. (5) to give

$$\Delta\Psi'_{ba}=\frac{1}{a}\Delta\Psi_{ap}+\Delta\Psi_{ba} \tag{6}$$

where $\Delta\Psi'_{ba}\equiv\Psi'^*_{ba}-\Psi'_{ba}$ and $\Delta\Psi_{ba}\equiv\Psi^*_{ba}-\Psi_{ba}$ and $\Delta\Psi'_{ap}$, $\Delta\Psi_{ap}$ are defined similarly. Since $\Psi_{ap}-\mathrm{TEP}=\Psi_{ba}$, after the basal solution change we have

$$\Delta\Psi_{ba}=\Delta\Psi_{ap}-\Delta\mathrm{TEP}|_{ba}. \tag{7}$$

Combining Eqs. (6) and (7) gives

$$\Delta\Psi'_{ba}=\left(1+\frac{1}{a}\right)\Delta\Psi_{ap}-\Delta\mathrm{TEP}|_{ba}. \tag{8}$$

Repeating the procedure leading up to Eq. (6), for a solution change at the apical membrane, we obtain:

$$\Delta\Psi'_{ap}=\Delta\Psi_{ap}+a\Delta\Psi_{ba}. \tag{9}$$

Combining Eqs. (7) and (9) gives

$$\Delta\Psi'_{ap}=(1+a)\Delta\Psi_{ap}-a\Delta\mathrm{TEP}|_{ap}. \tag{10}$$

Eqs. (8) and (10) link the experimental observables a, $\Delta\Psi_{ap}$, $\Delta\Psi_{ba}$ and ΔTEP with the quantities that are directly related to membrane conductance, $\Delta\Psi'_{ap}$ and $\Delta\Psi'_{ba}$.

Starting from the definition of Ψ'_{ap} in Eq. (2) it can be shown that

$$\Delta\Psi'_{ap}=\frac{g_{ai}}{\sum_i g_{ai}}(E^*_j-E_j) \tag{11}$$

where

$$E_j^* - E_j = \frac{RT}{F} \ln \frac{(C_j)_{\text{final}}}{(C_j)_{\text{initial}}}$$

and $(C_j)_{\text{initial}}$, $(C_j)_{\text{final}}$ are the concentrations of the j^{th} ion in the apical bath, before and after the change.

Therefore, if we plot $\Delta\Psi'_{ap}$ (or $\Delta\Psi'_{ba}$) as a function of $\log[C_i]$, we can obtain the *relative* conductance of that ion at each membrane but we cannot obtain g_{aj} or $\frac{1}{\sum_i g_{ai}}$. This requires that we also make a double-sided change in the concentration of the j^{th} ion. This experiment can be represented formally by putting asterisks on *all* the terms in Eq. (5). Subtracting Eq. (5) from Eq. (4) then gives

$$\Delta\Psi_{ap}|_D + a\,\Delta\Psi_{ba}|_D = \Delta\Psi'_{ap} + a\,\Delta\Psi'_{ba} \tag{12}$$

where $\Delta\Psi_{ap}|_D$ and $\Delta\Psi_{ba}|_D$ are the recorded changes in membrane potential when both baths are simultaneously changed. In analogy to Eq. (7)

$$\Delta\Psi_{ba}|_D = \Delta\Psi_{ap}|_D - \Delta\text{TEP}|_D. \tag{13}$$

Combining Eqs. (12) and (13) gives

$$\Delta\Psi'_{ap} = \Delta\Psi_{ap}|_D(1+a) - a\,\Delta\Psi'_{ba} - a\,\Delta\text{TEP}|_D. \tag{14}$$

In order to derive an expression for R_a we need another equation that connects $\Delta\Psi'_{ap}$, $\Delta\Psi'_{ba}$ and $\Delta\text{TEP}|_D$. Subtracting Eqs. (3a) and (3b) gives

$$\text{TEP} \equiv \Psi_{ap} - \Psi_{ba} = \Psi'_{ap} - \Psi'_{ba} - i(R_a + R_b) \tag{15}$$

and after a double-sided change

$$\Delta\text{TEP}|_D = \Delta\Psi'_{ap} - \Delta\Psi'_{ba} - \Delta i(R_a + R_b) \tag{16}$$

where, by Ohm's law

$$\Delta i = \frac{\Delta\Psi'_{ap} - \Delta\Psi'_{ba}}{R_a + R_b + R_s}. \tag{17}$$

Combining Eqs. (17) and (16) we obtain the desired relation

$$\Delta\text{TEP}|_D = \frac{R_s}{R_a + R_b + R_s}(\Delta\Psi'_{ap} - \Delta\Psi'_{ba}). \tag{18}$$

Substituting Eq. (18) into Eq. (14) we obtain

$$R_a = \frac{R_t}{\Delta\text{TEP}|_D}\left[\Delta\Psi'_{ap} - \Delta\Psi_{ap}|_D + \frac{a}{1+a}\Delta\text{TEP}|_D\right]. \tag{19}$$

All the quantities on the right, therefore, can be determined from the two experiments, a single- and double-sided ion concentration change; and once R_a is known, R_b and R_s can be calculated from a and R_t. If the surface area of these membranes can be estimated then the specific resistances can also be obtained.

There is another useful expression that also depends on the Case I assumptions. Starting with Eq. (15) and making an apical solution change

$$\Delta\text{TEP}|_{ap} = \Delta\Psi'_{ap} - \Delta i(R_a + R_b) \tag{20}$$

where

$$\Delta i = \frac{\Delta \Psi'_{ap} - \Delta E_s}{R_a + R_b + R_s}$$

and ΔE_s is the shunt battery produced by the single-sided change. Therefore,

$$\Delta \mathrm{TEP}|_{ap} = \Delta \Psi'_{ap} \left(\frac{R_s}{R_a + R_b + R_s} \right) + \Delta E_s \left(\frac{R_a + R_b}{R_a + R_b + R_s} \right). \tag{21}$$

This equation points out the relationship between ΔTEP, $\Delta \Psi'_{ap}$ and ΔE_s and was first used by Rose and Schultz (1971) in an analysis of the rabbit ileum.

Case II: a, R_s and R_t are Not *Constant*

Suppose that a solution composition change on the *basal* side alters a, R_s and R_t, the change in a resulting from a change in R_b, R_a staying constant. This assumption will be considered in more detail in the Results. Again, starting from Eq. (4):

$$\Psi_{ap} + a \Psi_{ba} = \Psi'_{ap} + a \Psi'_{ba}$$

and after the change

$$\Psi^*_{ap} + a^* \Psi^*_{ba} = \Psi'_{ap} + a^* \Psi'^*_{ba} \tag{22}$$

where *only* Ψ'_{ap} remains unaltered. Subtracting these two equations we have

$$\Delta \Psi_{ap} + a^* \Psi^*_{ba} - a \Psi_{ba} = a^* \Psi'^*_{ba} - a \Psi'_{ba}. \tag{23}$$

This equation has two unknowns, Ψ'^*_{ba} and Ψ'_{ba}, and we wish to know the difference, $\Delta \Psi'_{ba} = \Psi'^*_{ba} - \Psi'_{ba}$. Substituting $i = \dfrac{\mathrm{TEP}}{R_s}$ into Eq. (3b) gives

$$\Psi_{ba} = \Psi'_{ba} + \mathrm{TEP} \left(\frac{R_b}{R_s} \right) \tag{24}$$

and by knowing (R_b/R_s) Eqs. (23) and (24) can be used to calculate $\Delta \Psi'_{ba}$. Similarly, a single-sided *apical* solution change leads to the analogous equation

$$a \Psi^*_{ap} - a^* \Psi_{ap} + a\, a^* (\Delta \Psi_{ba}) = a \Psi'^*_{ap} - a^* \Psi'_{ap} \tag{25a}$$

and from (3a)

$$\Psi_{ap} = \Psi'_{ap} - \mathrm{TEP} \left(\frac{R_a}{R_s} \right). \tag{25b}$$

Again, knowing (R_a/R_s) one can determine $\Delta \Psi'_{ap}$.

It should be clear that the ion concentration changes that fall in the Case II category are difficult to analyze because the resistance ratios in Eqs. (24) and (25b) rarely can be directly obtained. For example, R_s could be calculated directly if an apical solution change only altered R_a. One could then measure R_t and a before and after the change and by applying Eq. (1) to each condition,

$$R_s = \frac{R_t R_t^* (a^* - a)}{R_t (1 + a^*) - R_t^* (1 + a)}. \tag{26}$$

R_a and R_b can then be calculated by using Eq. (1) and the measured values of R_t and a. However, if R_s also varies then Eq. (26) must be generalized to

$$R_s = \frac{R_t R_t^* [m(1+a^*) - (1+a)]}{R_t(1+a^*) - R_t^*(1+a)} \tag{27}$$

where m is the ratio of the shunt resistance before and after the solution change R_s/R_s^*. These equations were used by Reuss and Finn (1974) in an analysis of the toad urinary bladder epithelium. The use of Eq. (27) requires independent information about the value of m. Lacking this information, an alternative is to first calculate R_s from a set of ion concentration changes that satisfy the Case I assumptions. This value of R_s can then be used, to a good approximation, to analyze a different set of experiments: those that satisfy the Case II assumptions. In these experiments a and R_t are measured and once a value of R_s is assumed, R_a, R_b and m can be calculated along with the Case II voltage responses (Eqs. 23–25).

Results

Electrical Components of the Model

Cell Membrane and Transepithelial Potentials

In 345 cells and 67 tissues the mean Ψ_{ap} was -88 mV. Over 85% of the cells had resting potentials between -75 and -95 mV. For each cell Ψ_{ba} was depolarized with respect to Ψ_{ap} by the amount of the transepithelial potential (TEP). The mean TEP was 10 mV (range 8–20).

Resistance Ratios

The resistance ratios R_t and a were measured frequently throughout each experiment. They were obtained by passing 6 μA to give deflections of $\Delta\text{TEP}(IR_t)$ and $\Delta\Psi_{ap}$, $\Delta\Psi_{ba}$ ($\Delta\Psi_{ap}/\Delta\Psi_{ba} = a$). For a sample of 40 tissues, $R_t = 3900\,\Omega$ (range 2800–5500), and $a = 0.42$ (range 0.3–0.6).

In a majority of experiments a and R_t changed after a solution composition change. Although the circuit model is linear the observed resistance changes could originate from nonlinear I–V relations. Fig. 4 shows these relations for a typical cell. The voltage responses are linear to beyond ± 40 mV for the apical membrane, and ± 50 mV for the basal membrane. For both membranes the linearity extends beyond the range of membrane potential change caused by any solution composition change.

Evidence for Electrical Shunting

Electrical coupling of the cell membranes by the shunt R_s appears, experimentally, as a change in *both* membrane potentials, following a single-sided solution change (Boulpaep, 1967, 1971). We recorded the two

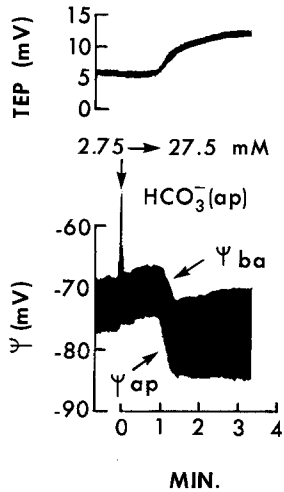

Fig. 5. Changes of both Ψ_{ap} and Ψ_{ba} produced by an ion concentration change on only one side. The arrows in the membrane potential trace (bottom) indicate that Ψ_{ba} and Ψ_{ap} are, respectively, the upper and lower borders of the trace. The width of the trace equals TEP plus 0.8 mV noise. The increase in apical $[HCO_3^-]_o$ (first arrow) rapidly and simultaneously hyperpolarizes both membrane potentials, $\Delta\Psi_{ap} = 10$ mV, and $\Delta\Psi_{ba} = 4$ mV. This increases TEP (upper record) from its low level of 6.6 mV in 2.75 mM $[HCO_3^-]$ to 12.6 mV; it appears also in the lower record as the widened trace

membrane potentials, at practically the same time, by electrically switching the reference for the microelectrode rapidly between the two solutions. In Fig. 5, elevating apical $[HCO_3^-]_o$ from 2.75 to 27.5 mM, isethionate substitution, hyperpolarized Ψ_{ap} by 10 mV and simultaneously hyperpolarized Ψ_{ba} by a smaller amount, 4 mV. This effect cannot be explained by leakage of HCO_3^- into the basal solution because the basal solution was continuously perfused with 2.75 mM HCO_3^-, and because the basal membrane is, itself, very insensitive to changes of basal $[HCO_3^-]_o$. In addition, elevating basal $[HCO_3^-]_o$ leaves the apical membrane potential unchanged. The effect of the shunt also can be demonstrated with 10^{-4} M ouabain, which is ineffective at the basal membrane (Steinberg & Miller, 1973). Upon placing it in the apical solution, however, both membrane potentials rapidly depolarized in unison, the apical greater than the basal (not shown).

Ion Concentration Changes

General

A survey of all the ions in the solution indicated that only changes in $[HCO_3^-]_o$ or $[K^+]_o$ significantly altered the membrane potentials at the

3-min measurement point (*see* Materials and Methods). Of the other ions, the largest responses were produced by changing apical or basal $[Na^+]_o$, but these were too small to quantify, about 1–3 mV for a 10-fold change. The Cl^- and Ca^{++} responses were still smaller. Also, 10-fold changes in $[Na^+]_o$, $[Cl^-]_o$ or $[Ca^{++}]_o$ did not significantly alter the resistance ratios, R_t and a.

Bicarbonate Responses

TEP. In the initial experiments the tissues were exposed to both phosphate and bicarbonate-CO_2-buffered solutions. It soon became clear that tissues exposed to the HCO_3^-—CO_2 solutions consistently showed higher transepitheial potentials and that the HCO_3^- sensitivity of the tissue was essentially limited to the apical side since changes in basal $[HCO_3^-]_o$ did not appreciably change TEP. Furthermore, the TEP seemed to increase as the $[HCO_3^-]_o$ in the apical solution was increased. That the effects attributable to HCO_3^- were not due to pH or, perhaps, to pCO_2, was supported by experiments in which the pCO_2 was varied while $[HCO_3^-]_o$ was kept constant. For example, equilibrating the 27.5 mM HCO_3^- solution with 70% O_2/30% CO_2 instead of 95% O_2/5% CO_2 produced a more than fivefold calculated increase in pCO_2 and a measured reduction of pH to 6.6, but did not change the TEP. Similarly, changing to 100% O_2 elevated the pH to 8.3 without affecting TEP. The removal of HCO_3^- from the 100% O_2 solution, however, rapidly decreased the TEP.

In these experiments HCO_3^- had been exchanged for Cl^-, so that part of the change in TEP might have resulted from the decrease in $[Cl^-]_o$. Experiments were performed, therefore, at a constant $[Cl^-]_o$ where HCO_3^- was exchanged for the less permeant isethionate ion. Pooled data from seven tissues are presented in Fig. 6. Above approximately 10 mM, the curve has a slope of 9.0 mV for a 10-fold increase in $[HCO_3^-]_o$.

Membrane Potential. Fig. 7*A* shows responses of apical membrane potential (lower panel) and TEP (upper panel) to 10-fold increases of $[HCO_3^-]_o$ in either the apical solution *alone* or in both the apical and basal solutions *together*. The voltage deflections that were elicited by transepithelial current pulses in order to monitor R_t and a, before and during each change, also are shown (Fig. 7*B*). The 10-fold increase in apical $[HCO_3^-]_o$ hyperpolarized Ψ_{ap} by 11 mV and increased TEP by 4 mV.

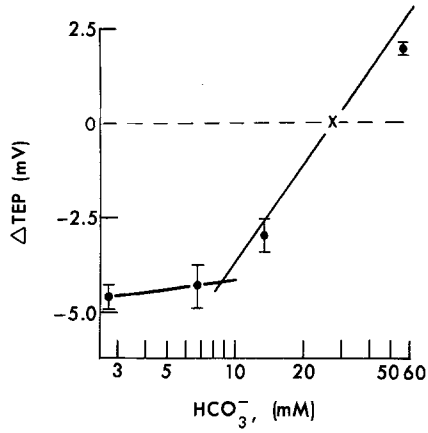

Fig. 6. TEP as a function of apical $[HCO_3^-]_o$; Cl^- constant at 32.1 mM, isethionate substitution. Data from seven tissues. Since TEP varied in the different tissues, range 7.5–12 mV, the HCO_3^- effects were plotted as ΔTEP's above and below the TEP of each experiment (interrupted line). Plotted are the means ±SEM

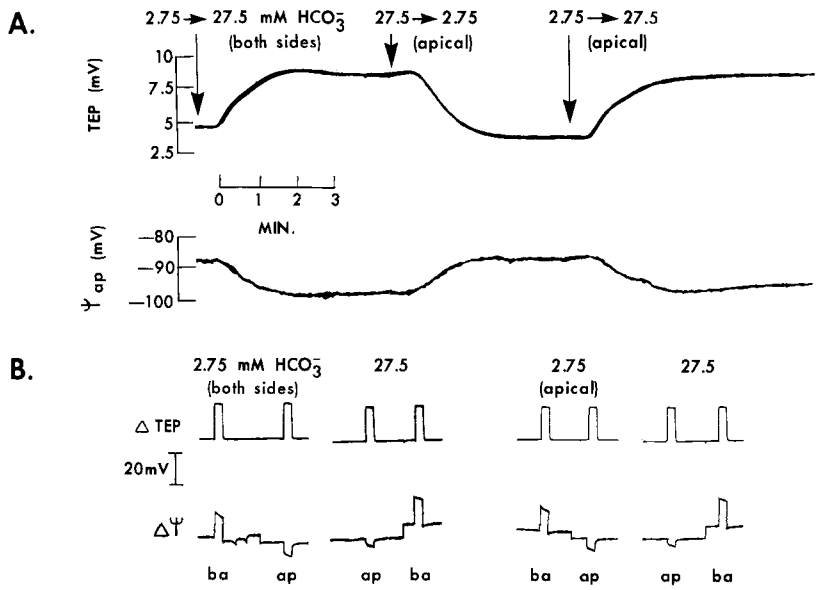

Fig. 7. Effect of changing $[HCO_3^-]_o$ on both sides or on the apical side alone; Cl^- substitution. All responses are from the same cell. (*A*) At the start there was 2.75 mM $[HCO_3^-]$ in both solutions and TEP = 4.8 mV (top), $\Psi_{ap} = -88$ mV (bottom), $R_t = 4100\,\Omega$, $a = 0.56$. After the $[HCO_3^-]_o$ of both solutions was increased to 27.5 mM (first arrow) the parameters changed at a latency of 30 sec, and levelled off within 3 min, so that Ψ_{ap} hyperpolarized by 11 mV, TEP increased by 4 mV, a decreased to 0.3 and R_t stayed constant. Returning *only* the apical solution to 2.75 mM $[HCO_3^-]$ (second arrow) returned all the parameters to their previous values; and increasing only the apical $[HCO_3^-]_o$ to 27.5 mM (third arrow) had the same effect as increasing it on both sides (first arrow). (*B*) Voltage deflections: ΔTEP (top); $\Delta\Psi_{ap}$, $\Delta\Psi_{ba}$ (bottom) in response to 6 μA transepithelial pulses

In order to apply the Case I analysis, we must first assess the extent to which a, R_t and R_s remain constant after the ion concentration change. The data of Table 1 show that R_t remained constant while the value of a shifted to a^* (column 3). Although statistically significant, the changes in a are small enough that they do not introduce appreciable error into the calculation of $\Delta\Psi_{ap}$ (column 8, Table 1; and Appendix). This error calculation also allowed a lower bound to be placed on the true value of R_s (column 9). This value is not significantly different from that *calculated* on the assumption that a (and R_s) remained constant after a HCO_3^- change (Table 1, part C). More direct evidence that R_s remained constant is that HCO_3^- changes on the basal side caused negligible changes in Ψ_{ba} and *no* change in a and R_t. Also, that R_t is constant no matter which anion (Cl^-, methylsulfate, isethionate) is substituted for HCO_3^- further supports this conclusion. If the shunt did distinguish between anions we would expect this to be reflected in a large change in R_t, especially since the *changes* in a are small (apical) or zero (basal). *Therefore, a Case I analysis of the HCO_3^- responses can be performed without introducing significant errors.*

Table 1 summarizes the experimental results and the $\Delta\Psi'_{ap}$ calculations for 10- and 20-fold changes in $[HCO_3^-]_o$ on the apical side alone or on both sides at the same time. To calculate $\Delta\Psi'_{ap}$ we used Eq. (10) and the a, ΔTEP and $\Delta\Psi_{ap}$ for each experiment. The average values of $\Delta\Psi'_{ap}$ for 10-fold and 20-fold increases in apical $[HCO_3^-]_o$ from 2.75 mM were, respectively, 14 and 19.5 mV. The values obtained when *both* solutions were changed, 13.4 and 20.4 mV, were not significantly different. These latter values were calculated from Eq. (14) assuming that $\Delta\Psi'_{ba}=0$. This was checked by directly calculating $\Delta\Psi'_{ba}$ in three experiments where apical and double-sided $[HCO_3^-]_o$ changes had been performed on the *same* cell. From these calculations $\Delta\Psi'_{ba}\approx 0$. Additionally, in experiments where basal $[HCO_3^-]_o$ was increased 20-fold (not shown) the maximum $\Delta\Psi_{ba}$ ever recorded was only 2 mV. $\Delta\Psi'_{ba}$, therefore, would be slightly larger and the error introduced by assuming $\Delta\Psi'_{ba}=0$ would be $a\,\Delta\Psi'_{ba}\approx 1$ mV.

Resistances. The data of Table 1 show that, to a good approximation, $\Delta\text{TEP}|_D=\Delta\text{TEP}|_{ap}$ and $\Delta\Psi'_{ba}=0$, and these equalities can be used in Eqs. (18) and (21) to demonstrate that $E_s=0$, so that

$$\Delta\text{TEP}|_{\text{apical}}=\left[\frac{R_s}{R_a+R_b+R_s}\right]\Delta\Psi'_{ap}. \tag{28}$$

Table 1. Summary of HCO_3^- data

Exp.	a	a^*	$R_t = R_t^*$ (KΩ)	ΔTEP (mV)	$\Delta\Psi_{ap}$ (mV)	$\Delta\Psi'_{ap}$ (mV)	Max. Error (mV)	R_s (KΩ)
A. 27.5⇄2.75 mM								
Apical (17,14)	0.44±0.04	0.66±0.05	3.44±0.15	5.1±0.5	11 ±0.4	14 ±0.6	<1.3±0.3	≧6.1±0.5
Both sides (4,3)	0.40±0.06	0.47±0.02	3.75±0.25	4.1±0.05	10.3±0.7	13.4±1.2		
B. 55⇄2.75 mM								
Apical (7,4)	0.36±0.04	0.58±0.11	3.6 ±0.23	8.9±0.9	15.7±0.8	19.5±1.2	<1.4±0.5	≧6.8±0.4
Both sides (6,4)	0.39±0.04	0.52±0.06	3.5 ±0.2	8.2±1.2	16.3±0.8	20.4±1		

C. Resistances calculated from HCO_3^- data

	R_a(KΩ)	R_b(KΩ)	R_s(KΩ)
Apical and both sides (7,5)	2.80±0.26	7.0 ±1.10	5.80±0.70
Apical (24,14)	3.56±0.25	6.48±0.47	6.38±0.45

The values in each column are mean ±SEM. In column 1 the numbers in parentheses refer to the number of cells and tissues, respectively. In part A, about half the apical experiments were methylsulfate substitutions, and the remainder were Cl^- substitutions. They can be analyzed together because they give the same voltage responses. Columns 8 and 9 were calculated as shown in the Appendix. In part B, methylsulfate is substituted for HCO_3^- ($[Cl^-]_o$ constant at 55 mM). Both sides of the tissue were initially bathed in 55 mM $[HCO_3^-]$ solution. The differences between columns 2 and 3, A and B, are statistically significant ($p<0.001$, and $p<0.01$, respectively). The differences for column 5, A, between apical and both-sided changes, are not statistically significant for a larger sample of tissues (10) and across the entire range of concentrations.

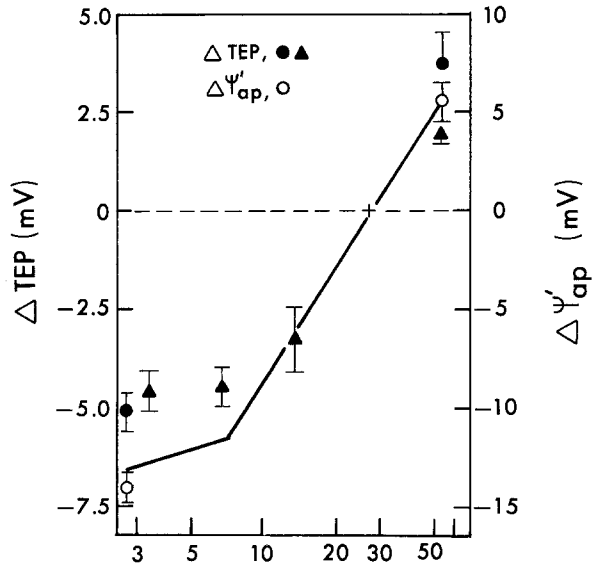

Fig. 8. $\Delta\Psi'_{ap}$ as a function of apical $[HCO_3^-]_o$. The data were taken from Table 1, methylsulfate and chloride substitutions: $\Delta\Psi'_{ap}$ (○), means and SEM's; and ΔTEP's (●), means and SEM's. Also included are the TEP data of Fig. 6 (▲). The solid line was calculated from Eq. (28) by using the TEP data and the average values of R_a, R_b and R_s in Table 1

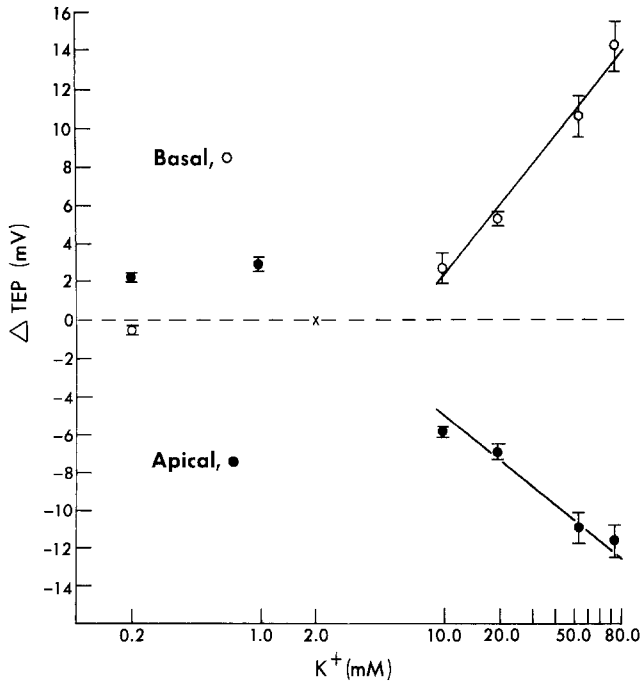

Fig. 9. TEP as a function of apical $[K^+]_o$ (●) and basal $[K^+]_o$ (○). The data from eight tissues are plotted as means ±SEM. Otherwise as in Fig. 6

Eq. (28) can be rewritten as

$$R_a = \frac{R_t}{\Delta \mathrm{TEP}|_{ap}} \left[\Delta \Psi'_{ap} - \Delta \Psi_{ap}|_{ap} + \frac{a}{1+a} \Delta \mathrm{TEP}|_{ap} \right]. \tag{29}$$

From Eq. (29), R_a can be calculated on the basis of only one experiment—a single-sided $[HCO_3^-]_o$ change. R_b and R_s are then calculated from the resistance ratios, a and R_t. The calculated resistances appear in Table 1 for 24 cells and 14 tissues. Also shown are the calculated resistances for seven experiments in which both the apical and double-sided $[HCO_3^-]_o$ changes were made on the same cell. Observe that the total shunt resistance R_s and the basal membrane resistance R_b are approximately equal and are about twice the resistance of the apical membrane R_a.

$\Delta \Psi'_{ap}$ vs. log$[HCO_3^-]_o$. Having calculated the resistances, Eq. (28) can be used to predict the magnitude of $\Delta \Psi'_{ap}$ from the *extracellular* response, ΔTEP (Fig. 8). This prediction, the solid line in Fig. 8, was based on the ΔTEP's of Fig. 6, which are replotted in Fig. 8 (▲). Notice also the agreement of the ΔTEP points from Table 1 (●) with the ΔTEP points of Fig. 6 (▲). That the *intracellular* data from Table 1 (○) lie along this line confirms the validity of Eq. (28). The position of the intracellular point at 55 mM HCO_3^- was confirmed in each case by also making 27.5 → 55 mM HCO_3^- changes. The slope of the line around 27.5 mM HCO_3^- (Fig. 6) is about 22 mV for a 10-fold change in apical HCO_3^-.

Potassium Responses

TEP. The data of Fig. 9 show the variations of TEP as a function of apical (●) or basal (0) $[K^+]_o$. For the apical side, the straight-line portion has a slope of 7 mV per 10-fold change in concentration, and the curve is linear from 1 to 84 mM. For basal solution changes the straight-line portion is linear from about 10 to 84 mM and has a slope of 13 mV per 10-fold change.

Membrane potential. Fig. 10 shows the response of membrane potential to large increases, 2 → 55 mM K^+, in either the apical (Fig. 10*IA*) or basal (Fig. 10*IIA*) solution for one cell. When the apical $[K^+]_o$ was elevated, Ψ_{ap} rapidly depolarized by 25 mV, while a similar elevation of basal $[K^+]_o$ rapidly depolarized Ψ_{ba} by 30 mV. In both cases there were simultaneous changes in TEP.

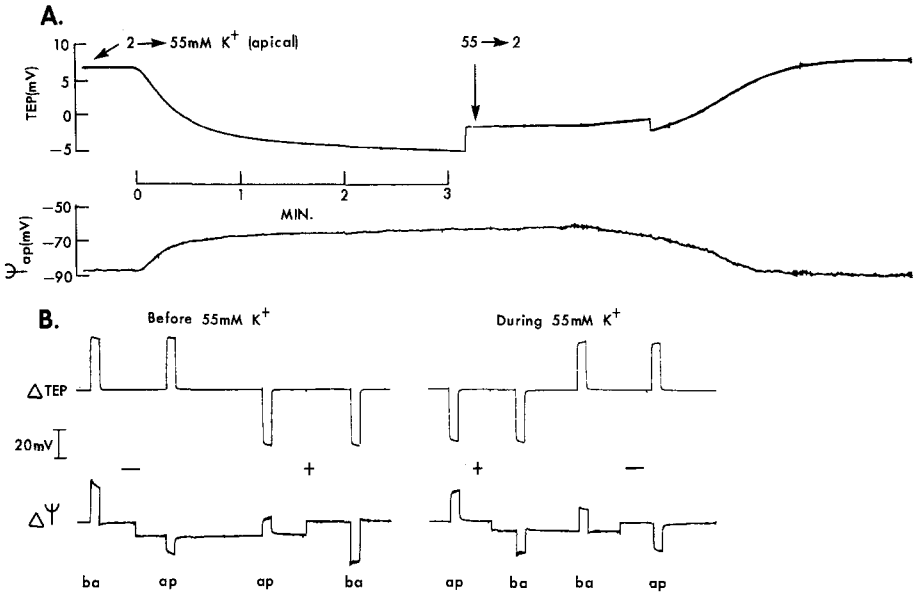

Fig. 10:*I*. Effects of a 27.5-fold increase in apical $[K^+]_o$. (*A*) TEP (top), Ψ_{ap} (bottom). In 2 mM K^+, TEP = 7.9 mV, $\Psi_{ap} = -88$ mV, $R_t = 3500\,\Omega$, $a = 0.5$. The increase to 55 mM K^+ (first arrow) depolarized the apical membrane by 25 mV and decreased TEP by 12 mV; R_t decreased to 3000 Ω and a increased to 1.4 (a^*). The return to 2 mM K^+ (second arrow) returned all values to their original levels (but $\Delta\Psi_{ap} = 28$ mV). Note there was a 1′50″ period in the TEP record (55→2) where the gain was quartered. (*B*) Voltage deflection ΔTEP, $\Delta\Psi_{ap}$ and $\Delta\Psi_{ba}$ in response to ±6 μA

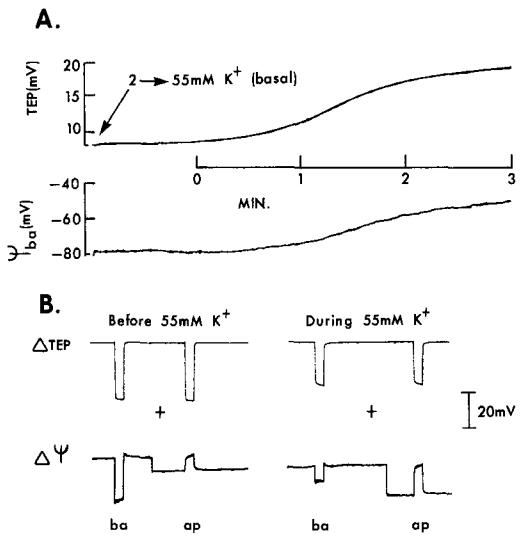

Fig. 10:*II*. Effect of a 27.5-fold increase in basal $[K^+]_o$. Format the same as Fig. 10*I* and from the *same* cell. The increase to 55 mM $[K^+]$ (arrow) depolarized Ψ_{ba} by 30 mV, increased TEP by 9.9 mV; R_t decreased from 3600 to 2400 Ω and a increased from 0.4 to 1.8 (a^*)

Resistances. The voltage deflections in Fig. 10, *IB* and *IIB* show that $[K^+]_o$ elevations on either side decrease R_t and increase a, the basal effects being larger. The time course of the changes in a and R_t, both onset and return, always paralleled the time course of the membrane potential changes. The magnitude of these changes are much larger than those induced by changes in $[HCO_3^-]_o$. For example, on the basal side a increased from 0.4 in 2 mM K^+ to 1.8 (a^*) in 55 mM K^+ (Fig. 10*IIB*).[1]

In order to calculate the changes in membrane resistance from the K^+ data we have relied on Eq. (27), the observed changes in R_t and a, and the mean value of R_s determined from the HCO_3^- data (Tables 1 and 2). We find, on the average, that a 10-fold increase in apical $[K^+]_o$ increases R_a from 3500 to 7000 Ω and decreases R_s from 6400 to 5000 Ω.

---

1 It is important to identify the locations and causes of the resistance changes that are indicated by the changes in a and R_t. The $[K^+]_o$ changes, for example, could osmotically alter the intracellular concentrations and/or the permeabilities of either cell membrane (Casteels, Droogman & Hendrickx, 1971). We believe that this effect is minimal because in five cells we were able to record 90% of the voltage change within 20 sec of the start of the change. The flow rate in these experiments was 15–18 cc/min and the maximum voltage, at 3 min, did *not* differ from the above experiments (Fig. 10, Table 2). We repeated these fast flow experiments for HCO_3^- changes and also were able to record the full potential in about 20 sec. We also monitored a, R_t and membrane potential while making 50% changes in osmolarity on either the apical or basal side (sucrose addition). Since there were no significant changes in these parameters within a 5 min observation period we concluded that the K^+ and HCO_3^- effects at the 3 min observation time did not have an osmotic basis. This conclusion has been directly tested for K^+ changes by Dr. Burks Oakley working in this laboratory. He placed double-barreled K^+-specific microelectrodes into these cells and found that intracellular K^+ changes were not in evidence (±5 mM) at 3 min.

Regarding locations of resistance changes, the change in a, although produced by new voltage drops across *both* cell membranes, does not necessarily indicate new resistances at both membranes. A change in the resistance of *one* cell membrane will alter the voltage drops at *both* membranes by altering the fraction of constant current that flows across the cell. Our evidence actually suggests that the resistance of the opposite cell membrane remains constant for single-sided $[K^+]_o$ changes; that R_b remains constant when apical $[K^+]_o$ is elevated and that R_a remains constant when basal $[K^+]_o$ is elevated. This is supported by the osmotic experiments just described, by the invariance of the apical HCO_3^- response to changes in *basal* $[K^+]_o$ and also by experiments in which $[K^+]_o$ on both sides was simultaneously changed. For example, if basal $[K^+]_o$ is elevated from 2 to 55 mM, a increases by a factor of 4.5. If an appreciable part of this increase were due to an increase in R_a and, more specifically, to a decrease in apical g_k then, by Eq. (2), the both-sided apical voltage response should be significantly smaller than the single-sided apical response. Actually, the both-sided response is a few mV's larger, a result that can be explained by changes in shunt current. In the both-sided case the shunt current stays approximately constant because both membranes depolarize in unison and by about the same amount. In the single-sided case the shunt current decreases, thereby hyperpolarizing the apical membrane and *reducing* the size of the diffusion potential.

A 10-fold increase in basal $[K^+]_o$ decreases R_b from 6400 to about 2300 Ω. For basal $[K^+]_o$ changes, Eq. (27), with a, a^* replaced by $1/a$, $1/a^*$, gives a value of m very close to one, suggesting that the resistance of the shunt is insensitive to changes in basal $[K^+]_o$ (Table 2).

$\Delta\Psi'_{ap}$ and $\Delta\Psi'_{ba}$ vs. log$[K^+]_o$. Table 2 summarizes the experimental results and calculations of $\Delta\Psi'$ for 20-fold increases in apical or basal $[K^+]_o$. In these experiments, the values of $\Delta\Psi'_{ap}$ and $\Delta\Psi'_{ba}$ were calculated by using Eqs. (23–25 and 27) and the data of Table 2. Fig. 11 presents the major results of this analysis, the plots of $\Delta\Psi'_{ap}$ (△) and $\Delta\Psi'_{ba}$ (○) *vs.* log$[K^+]_o$. The closed symbols represent the ΔTEP data that were also obtained in these experiments.

The open circles in the $\Delta\Psi'_{ba}$ plot of Fig. 11 are the data calculated, above, from direct measurements of $\Delta\Psi_{ba}$. They show that decreasing basal $[K^+]_o$ below 2 mM has little effect on $\Delta\Psi_{ba}$, less than 1 mV per 10-fold change, while the voltage change per 10-fold increase in basal $[K^+]_o$ increases near 20 mM from 24 to 52 mV. This result was corroborated by the calculation of intervening $\Delta\Psi'_{ba}$ points, the open squares, from the ΔTEP data of Fig. 9.[2]

The slope of the apical membrane curve above 20 mM K^+ is less than that of $\Delta\Psi'_{ba}$, 38.5 mV compared to 52 mV per 10-fold change in concentration. $\Delta\Psi'_{ap}$ increases above 20 mM, from 30 to 38.5 mV, but this increase is much smaller than the basal increase and is within the variability of the measurements. A 10-fold reduction in apical $[K^+]_o$ hyperpolarizes Ψ'_{ap} by 11 mV. This response is much larger than the basal

---

2 In this calculation the Case I analysis (Theory section) was applied to small increments and decrements of basal $[K^+]_o$ around the 20 and 55 mM data points (○). The difference in TEP between two basal $[K^+]_o$ concentrations is given by

$$\Delta\text{TEP}_{\text{basal}} = -\Delta\Psi'_{ba}\left[\frac{R_s^*}{R_a+R_b^*+R_s^*}\right]+\Delta E_s\left[\frac{R_a+R_b^*}{R_a+R_b^*+R_s^*}\right]$$

where $\Delta\Psi'_{ba}$ is the difference in the basal membrane battery and ΔE_s is the difference in the shunt battery. Now, ΔE_s can be ignored because it is very small, even for the large changes in basal $[K^+]_o$ (*see below*). Therefore

$$-\Delta\Psi'_{ba} \cong \Delta\text{TEP}\left[1+\frac{1+1/a^*}{R_s^*/R_a}\right].$$

The ΔTEP values can be taken from Fig. 9 because the slope of this curve agrees well with the ΔTEP of Fig. 1, the 2 mV difference being within the variability of the measurement. The values of a^*, R_s^* and R_a are those that were obtained for the 20 and 55 mM points (Tables 1 and 2). They can be used because small changes in basal $[K^+]_o$ about these points will alter the resistance parameters very little.

Table 2. Summary of K^+ data

Exp.	a	a^*	R_t (KΩ)	R_t^* (KΩ)	ΔTEP (mV)	$\Delta\Psi$ (mV)	$\Delta\Psi'$ (mV)	m
A. $2 \rightleftarrows 20$ mM								
Apical (20,12)	0.40 ± 0.04	0.83 ± 0.07	3.7 0.30	3.3 ± 0.27	9.5 ± 0.50	23.8 ± 1.1	29.7 ± 1.3	1.28 ± 0.03
Basal (20,12)	0.37 ± 0.04	1.04 ± 0.09	3.34 ± 0.13	2.57 ± 0.04	6.7 ± 0.40	18.4 ± 1.3	24.5 ± 1.8	0.91 ± 0.08
B. $2 \rightleftarrows 55$ mM								
Apical (11,9)	0.39 ± 0.05	1.29 ± 0.10	3.58 ± 0.11	3.06 ± 0.11	15.1 ± 0.60	31.9 ± 2.6	45.3 ± 3.2	1.43 ± 0.04
Basal (11,7)	0.37 ± 0.04	1.65 ± 0.17	3.9 ± 0.12	2.76 ± 0.08	13.8 ± 0.40	35.2 ± 2.2	46.5 ± 2.2	0.94 ± 0.08
C. $2 \rightleftarrows 0.2$ mM								
Apical (8,5)	0.32 ± 0.05	0.15 ± 0.03	3.5 ± 0.07	3.78 ± 0.04	2.25 ± 0.20	9.2 ± 0.8	11.4 ± 1	0.96 ± 0.07

The values in each column are mean ± SEM. In column 1 the numbers in parentheses refer respectively to the number of cells and tissues. The differences between a, a^* (columns 2, 3) and R_t, R_t^* (columns 4, 5) are all significant, at the $p < 0.001$ level (paired t-est). The apical and basal m values are also significantly different, $p < 0.001$, as are the values for $2 \rightarrow 20$ mM *vs.* $2 \rightarrow 55$ mM changes, $p < 0.01$.

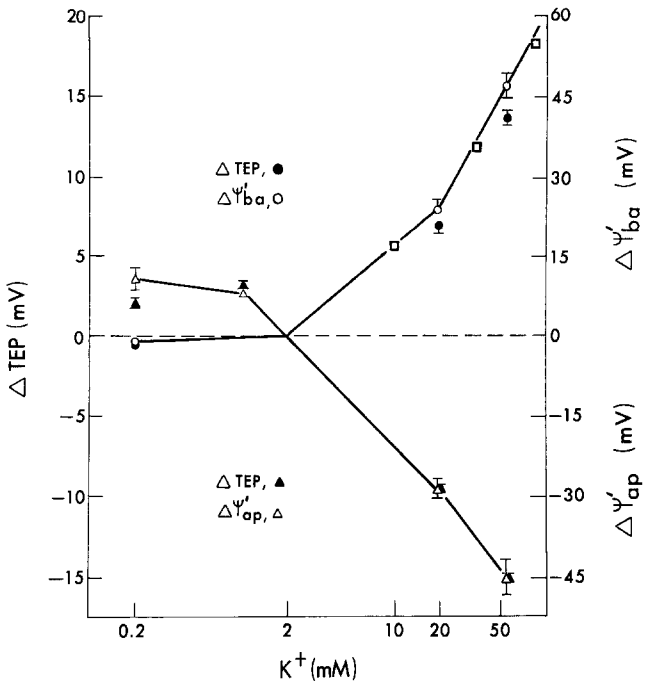

Fig. 11. $\Delta\Psi'_{ba}$ (top) and $\Delta\Psi'_{ap}$ (bottom) as a function of $[K^+]_o$. The means and SEM's for $\Delta\Psi'_{ba}$ (○) and $\Delta\Psi'_{ap}$ (△) were taken from Table 2. The ΔTEP's, ●, ▲, for these experiments also are plotted. The solid lines connect the intracellular data points. The open squares are calculated as described in the text. The value of $\Delta\Psi'_{ap}$ at 1 mM was calculated from a series of TEP measurements between 1 and 2 mM that gave $\Delta\text{TEP} = 3.0 \pm 0.3$ mV (7 tissues). The rationale for this calculation is given in footnote 2

membrane response as shown here and in the TEP data of Fig. 9. It is possible to explain this difference and the slope change of $\Delta\Psi'_{ba}$ near 20 mM K^+, in part, by the action of the choroid as a large unstirred layer (*see* Materials and Methods and Discussion).

Possible Electrogenic Contributions to the Voltage Responses

We have tentatively identified a Na—K pump on the apical membrane by its sensitivity to ouabain (Steinberg & Miller, 1973) and experiments are now in progress to establish its electrogenicity. When placed in the apical solution ouabain, 10^{-4} M, depolarizes Ψ_{ap} by 8–10 mV. The effect begins within 30 sec and is 90% complete within 6 min. At 15 min we noticed the onset of a second phase of depolarization which contained for several hours at 0.4 mV/min. This was probably due

to ion concentration gradients running down. Even if there is an electrogenic contribution to the resting state there need not be a significant electrogenic contribution to the voltage responses if, for example, the membrane resistance is sufficiently low or if the electrogenic contribution is voltage dependent (Kostyuk, Krishtal & Pidoplichko, 1972).

In the theory section we assumed that the calculated values of $\Delta\Psi'_{ap}$ and $\Delta\Psi'_{ba}$ resulted solely from diffusion potentials. The calculation of relative conductance, however, would be in error if a significant part of the observed potential changes were contributed by electrogenic pumps. If the pump is hyperpolarizing, with a rate monotonically related to apical $[K^+]_o$, then in high $[K^+]_o$ it would partially mask the depolarizing diffusion potential; and this effect would be enhanced by the observed K^+-dependent increase in R_a. We estimated that the electrogenic contributions to the apical K^+ membrane voltage responses were small by comparing response magnitudes before and 10 min after the application of 10^{-4} M ouabain. The differences at high concentrations were only 2–3 mV out of 26 mV (55 mM apical K^+) and they were negligible at low concentrations (0.2 mM K^+). For HCO_3^- there is no specific pump inhibitor; g_{HCO_3} (*see* p. 28) is, therefore, an apparent conductance.

It is worth noting that the calculation of R_a in Eq. (29) will be the same even if the membrane voltage response is partially electrogenic. This follows from Eq. (28) which shows that $\Delta\Psi'_{ap}$ and ΔTEP are directly proportional. This relationship is valid regardless of the origin of the membrane potential change.

Transepithelial Resistance and Potential

Knowing Ψ_{ap}, TEP and the resistances, Ψ'_{ap} and Ψ'_{ba} can be calculated from Eqs. (24) and (25b). For a sample of 30 cells from 20 tissues the average value of Ψ'_{ap} is -96.8 mV ± 1.5 and Ψ'_{ba} is -69 mV ± 1.5. The difference, 27.8 mV, is the TEP that should be observed if the shunt resistance was infinite. This follows from Eqs. (1) and (3) rewritten as:

$$\text{TEP} = \frac{(\Psi'_{ap} - \Psi'_{ba})\, R_t}{R_a + R_b}.$$

Since the shunt resistance is finite, the TEP's that we observe are smaller by a factor of 1.8–2.8; they are typically 10–15 mV instead of 27.8 mV. Most of the variability in R_t and TEP is probably due to the variation in edge damage caused by the mechanical seal. The largest R_t we have

observed is about 9000 Ω and if $R_a + R_b \approx 10{,}000\,\Omega$ (Table 1) then the TEP should have been 25 mV. In fact, the observed TEP was 20 mV, which is within the combined error of these measurements and suggests that R_s can be very large. The consistency of these results can also be tested by calculating a value for $R_a + R_b$ using 27.8 mV and the observed R_t and TEP from a large number of tissues not studied with microelectrodes. For 84 tissues $R_a + R_b = 10{,}800\,\Omega \pm 2000$ (*SD*), in good agreement with the results of Table 1.

The Shunt

Resistance

The results of Table 1 show that, on the average, R_s is about 6000 Ω, and $R_a + R_b \approx 10{,}000\,\Omega$. We estimate that the specific resistance of $R_a + R_b$ lies between 6400 and 8200 Ω cm^2 (*see* Discussion) and comparing this value to 10,000 Ω gives an equivalent transepithelial area for $R_a + R_b$ of 0.64–0.82 cm^2. For a tissue with $R_t = 4000\,\Omega$ and an equivalent area of 0.73 cm^2, the specific resistances of: $R_a + R_b \approx 7300\,\Omega$ cm^2, $R_t \approx 3000\,\Omega$ cm^2 and $R_s \approx 5100\,\Omega$ cm^2. The value of R_t in some tissues, however, has been as high as 9000 Ω so that $R_s \approx 66{,}000\,\Omega$ cm^2. In this case the shunt resistance is almost a factor of 10 larger than the cellular resistance and that classifies the pigment epithelium as a "tight" epithelium (Frömter & Diamond, 1972). Note that this conclusion is unchanged even if the specific resistance of $R_a + R_b$ lies outside the range given above.

Voltage

When an ion concentration change occurs on one side of the tissue both shunt pathways may develop batteries. The edge battery would be a small liquid junction potential of a few mV or less; its actual magnitude calculable from the composition of the solutions bathing each side of the tissue (Barry & Diamond, 1970). The paracellular battery probably would be a membrane diffusion potential and it could be large depending on the permeability of the pathway. Its full magnitude would not appear in the transepithelial potential, however, since it would be shunted by the edge pathway in the same manner as the cell membrane batteries. This reduces the measured contribution from these batteries to the TEP by 50–65% (above). Two observations indicate that the shunt does not distinguish between anions (HCO_3^-, Cl^-, methylsulfate, isethionate). First, $E_s = 0$, independent of the ion substituted for HCO_3^-, and second,

as mentioned previously, R_t is constant no matter which anion is substituted for HCO_3^-, (Table 1, Figs. 5–8).

In the case of apical $[K^+]_o$ changes the shunt *does* distinguish between K^+ and Na^+, as evidenced in Table 2 by m values that do not equal one. If we treat the edge pathway as a liquid junction of fixed volume, R_s/R_s^* can also be calculated from the mobilities and concentrations of the ions before and after the solution changes (MacInes, 1961). In this case R_s/R_s^* is 1.02, significantly smaller than the value of m demanded by the data of Table 2. This suggests that the variation of R_s with $[K^+]_o$ occurs via another pathway, probably the paracellular one. The E_s's calculated for these experiments are small: 0.4 mV ± 0.22 for 2 to 20 mM and 2.2 mV ± 0.3 for 2 to 55 mM. They are calculated by using the Case II version of Eq. (21). A contribution from the edge cannot by ruled out, however, especially since the calculated liquid junction potentials, 0.6 and 2.2 mV, are in the same range as the calculated E_s's.

For basal $[K^+]_o$ changes m is very close to one for all concentrations (Table 2) and E_s is approximately zero. This result might point to an asymmetry in the shunt pathway, but it is also possible that, in some way, the K^+ ions have more difficulty penetrating R_s from the basal side.

Discussion

When mounted in a perfusion chamber, the apical and basal membranes of the frog pigment epithelium are electrically coupled. A significant fraction of the voltage change produced at one membrane shunts to the opposite side and, therefore, a correction must be applied in order to estimate the relative conductance. Considering the anatomy of this tissue the simplest model capable of analyzing the voltage responses was presented in Fig. 4. With this model we determined the relative conductances of the apical and basal membranes, the input resistances of these membranes and the shunt, and estimated their specific resistances. Since the basal membrane, at high $[K^+]_o$, is very nearly a K^+ electrode we could also estimate the intracellular K^+ concentration. These results will be discussed, beginning with the apical membrane.

Apical Membrane

Resistance. The apical membrane's resistance can be altered by changes in apical $[K^+]_o$ or $[HCO_3^-]_o$. The HCO_3^- concentration changes

have almost no effect on R_t but do cause a small but significant rise in a (Table 1). HCO_3^--sensitive voltage and conductance changes are unusual but have been observed in other tissues (Woodbury, 1971; Spenny *et al.*, 1975). By comparison, the K^+ concentration changes cause large changes in membrane resistance. Raising apical $[K^+]_o$ increases a and decreases R_t; lowering $[K^+]_o$ from $2 \rightarrow 0.2$ mM has the opposite effect. The direction of these K^+ resistance changes are not without precedent. Elevation of $[K^+]_o$, for example, at the mucosal membrane of frog stomach (Spangler & Rehm, 1968) and at the surface cells in *Necturus* fundic gastric mucosa (Spenny *et al.*, 1974) also decreases R_t and appears to raise the resistance of the membrane facing the elevated $[K^+]_o$. When external $[K^+]_o$ is lowered there is direct evidence from combined conductance and flux measurements in taenia coli cells that the potassium permeability rises (Casteels *et al.*, 1971).

From the comparison of single and both sided K^+ changes we concluded that the rise in a that occurs when apical $[K^+]$ is elevated signals an increase in R_a, and hence a decrease in apical conductance. This decrease may be occurring in the K^+ channel, in the HCO_3^- channel or in both channels. In additional experiments these alternatives were tested by making 10-fold changes in apical $[HCO_3]_o$ in the presence of 2 or 55 mM K^+. By Eq. (11), if potassium was *only* affecting the HCO_3^- channel then the HCO_3^- diffusion potential should be much smaller in the high $[K^+]_o$ solution, while it should be much larger if the effect was only on the K^+ channel. An intermediate result would be produced if both channels were affected. Our finding, that the diffusion potentials are only 20–30% larger in 55 mM K^+, suggest that both channels are affected. This needs further testing, for example, by the effect of pH and divalent cations on the K^+ channels (Wright & Diamond, 1968; Hagiwara, Fukuda & Eaton, 1974).

Voltage responses. From the slopes of the HCO_3^- and K^+ curves (Figs. 8 and 11, respectively), and the voltage response to 10-fold reduction in apical $[Na^+]_o$ we estimate for the apical membrane that $T_K \approx 0.52$, $T_{HCO_3} \approx 0.39$, $T_{Na} \approx 0.05$. [In contrast, the directly measured membrane potential changes, $\Delta \Psi_{ap}$ (Table 2), give the incorrect values of $T_K \approx 0.30$ and $T_{HCO_3} \approx 0.24$.] The apical K^+ curve in Fig. 11 is nearly linear between 1 and 55 mM, the deviation from linearity being within the error of the measurements. This has been checked in individual cells by making successive $2 \rightarrow 20$ mM, $2 \rightarrow 33$ mM and $2 \rightarrow 55$ mM K^+ changes. This linearity could be due to the membrane conductances remaining approx-

imately constant with increasing K^+ concentration but the large changes in a (Table 2) that occur when $[K^+]_o$ is elevated make this explanation unlikely. Alternatively, the K^+ conductance (g_K) could be much larger than the combined conductances of all other ions. In that case the slope of the $\Delta\Psi_{ap}$ line should be very close to 58 mV, but it is only 38.5 mV. Following Hodgkin and Horowicz (1959), a third possibility is that $E_K \approx E_{HCO_3^-}$. This is supported by constant product experiments (data not shown), $[K^+]_o \cdot [HCO_3^-]_o = 55\,\text{mM}^2$, in which there is a linear relation between membrane potential and $\log[K^+]_o$ (or $\log[HCO_3^-]_o$) with a slope of about 55 mV. Against this is the basal membrane data which gives $E_K \approx E_{HCO_3^-} = -100\,\text{mV}$ and therefore would predict an intracellular pH of 5.66, more than a pH unit lower than is measured in most cells (Paillard, 1972; Thomas, 1974; Aickin & Thomas, 1975). Another explanation, perhaps more likely, is that g_K changes with K^+ concentration and the remaining membrane conductance, mostly $g_{HCO_3^-}$, changes also, and by about the same percentage as g_K. In this way the relative K^+ conductance T_K would remain nearly constant and the $\Delta\Psi'_{ap}$ curve approximately linear.[3]

The slope T_K of the $\Delta\Psi'_{ap}$ curve decreases between 1 and 0.2 mM (Fig. 11). This could result from a relative increase in $g_{HCO_3^-}/g_K$ and/or g_{Na}/g_K as suggested by the decrease in a (Table 2), which we have taken to indicate an increase of the apical membrane conductance.

Basal Membrane

Voltage responses. The relative potassium conductance T_K of the basal membrane (Fig. 11) increases as a function of $[K^+]_o$ and there are two major changes in slope, the first around 2 mM K^+ and the second near 20 mM K^+. We are faced with the problem of understanding these slope changes. First, consider the change near 2 mM where the decrease in basal

3 As a corollary we can reject the idea that *only* g_K (or g_{HCO_3}) changes with K^+ concentration. From the values of a at 2, 20 and 55 mM we calculate T_i^* ($i = K^+$, Na^+, HCO_3^-) in 20 and 55 mM K^+, and then predict the $\Delta\Psi'_{ap}$ data in Fig. 11. From Eq. (2)

$$\Delta\Psi'_{ap} = T_K^* E_K^* - T_K E_K + E_{HCO_3}(T_{HCO_3}^* - T_{HCO_3}) + E_{Na}(T_{Na}^* - T_{Na})$$

and from the basal membrane data $E_K = -100\,\text{mV}$. The value of E_{HCO_3} is allowed to range from -20 to -100 mV and E_{Na} can range between 0 and 60 mV. Over this range and for all the experiments summarized in Table 2 the calculated values of T_i^* lead to values of $\Delta\Psi'_{ap}$ which are about the same (within a few mV's) for 2→20 mM and 2→55 mM changes. These calculations, therefore, strongly reject the idea that only one conductance mechanism is altered by increasing K^+ concentration.

$[K^+]_o$ from 2→0.2 mM led to only a $\Delta\Psi'_{ba}$ of 1–2 mV at 3 min. This cannot be explained by a decrease in basal membrane K^+ conductance, since a remained constant. A more likely explanation is that the basal membrane did not see the full concentration change at 3 min. This hypothesis has recently been confirmed by Dr. Burks Oakley, working in this laboratory. He placed K-specific microelectrodes just outside the basal membrane and found that only a small fraction (10–20%) of the final concentration change had occurred at 3 min.

Obviously it is the choroid that prevents the cell membrane from "seeing" the full change, for example, by causing a diffusion delay. For a 2→0.2 mM K^+ change the diffusion equation can be used in Eq. (11) to calculate a value of T_K (at 2 mM) that is consistent with the observed $\Delta\Psi'_{ba}$.[4] This calculation shows that a diffusion delay through the unstirred layer cannot entirely account for the small size of $\Delta\Psi'_{ba}$. Another mechanism that would also slow the change is the emission of sufficient K^+ from the intracellular compartment of the choroid.

In contrast to the 2→0.2 mM K^+ change, the 2→55 mM K^+ change caused a large alteration in a (0.4→1.7). The increase in slope near 20 mM may therefore be caused by an increase in g_K, but this increase cannot be solely explained by a conductance increase since diffusion delays also occur for 2→55 mM K^+ changes.[4] (This has also been confirmed by Dr. Oakley with K-specific microelectrodes.)

---

4 The choroid acts as a large unstirred layer whose diffusion properties determine, for any change in concentration of the bulk solution, how fast the concentration gradient at the basal membrane will change. The time course can be calculated from the diffusion equation knowing the thickness of the choroid (~150 μ) and the effective diffusion coefficient. The time course of the voltage response is then obtained by using Eq. (11) (Kidder, Cerejido & Curran, 1964; Spangler & Rehm, 1968). For this calculation we assume that the effective K^+ diffusion coefficient is 10% of its free solution value of 1.6×10^{-6} cm²/sec (Kidder *et al.*, 1964; Spangler & Rehm, 1968). We find that $\Delta\Psi'_{ba} = 48\, T_K$ and therefore $T_K \approx 0.02$–0.04, more than an order of magnitude smaller than the observed slope at 2 mM. In order to predict the slope at 2 mM we would have to assume a K^+ diffusion coefficient that is 1% of its free solution value, but that is an order of magnitude smaller than that deduced from other epithelia (Kidder *et al.*, 1964; Diamond, 1966; Spangler & Rehm, 1968).

The change in slope, near 20 mM, cannot be totally explained by an increase in g_K. Assuming that the change in a (0.4→1.65) that occurred with a 2→55 mM K^+ change originated solely from a change in basal membrane conductance, G_b, then the following relations hold:

$$\frac{a}{a^*} = \frac{G_b}{G_b^*}, \qquad G_b^* - G_b = g_K^* - g_K, \qquad \frac{T_K}{T_K^*} = \frac{G_b^* g_K}{G_b g_K^*}$$

and finally, with a little algebra, $T_K = (4.1)\, T_K^* - 3.1$. In the vicinity of 55 mM K^+, $T_K^* = 0.9$ and the last equation predicts a $T_K(2\text{ mM}) = 0.59$, which is much larger than actually observed.

Above 20 mM K^+ the slope remains constant and, as mentioned previously, this was checked in individual cells by making successive 2→20, 2→33 and 2→55 mM K^+ changes. Consequently, we have used the slope of the $\Delta\Psi'_{ba}$ curve *above* 20 mM K^+ (52 ± 3 mV per decade) rather than the poorly defined slope around the reference point to calculate a T_K of 0.9 for the basal membrane. We think that this may be justified because the basal membrane potential showed no appreciable response to changing the concentration (10-fold) of *any ion* except potassium, and because the diffusion delays are probably much more effective in reducing the slope at the lower concentrations.

Resistances. The apical membrane resistance R_a (Table 1) is approximately 3500 Ω. From TEM (Nilsson, 1964) and SEM photographs (Steinberg, 1973) we estimate that the apical processes enlarge the geometrical area (0.07 cm^2) by a factor of about 30. (This was arrived at by counting the number of apical processes per cell and by observing that each process approximated a right circular cone of height 60 μ with a base diameter of 2.5 μ and a tip diameter of 0.5 μ.) This means that the specific resistance is about 6000–7000 Ω cm^2, about 50% larger than the values reported for the apical membrane of several other epithelia (Frömter, 1972; Reuss & Finn, 1974; Spenny *et al.*, 1975).[5]

The calculated basal membrane resistance R_b is about 6400 Ω (Table 1) and we estimate that the geometrical area (0.07 cm^2) is, at most, increased by a factor of three by the sparse basal infoldings (Kuwabara, *in press*). This means that the specific resistance is about 450–1200 Ω cm^2 and, therefore, the specific resistance of $R_a + R_b$ could be as large as 8200 Ω cm^2.

Intracellular ion concentration. For a sample of 30 cells (20 tissues) the average basal resting membrane potential Ψ_{ba} is about 82 mV, inside negative, and the average value of Ψ'_{ba} is $-69 \text{ mV} \pm 1.5$. The average value of T_K *above* 20 mM is 0.90, but it increases slightly, as judged from

5 It was not possible to study the electrical properties of the apical processes. We treated them as extensions of the apical membrane with an internal resistance that is small compared to the plasma membrane resistance. If the peripheral portions of these processes have a sufficiently short space constant, then the area correction factor of 30 may be too large. If we consider only the cone frustrum defined by diameters of 2.5 and 1 μ its area constitutes 83% of the total cone area. Even if we assume that the specific resistance is a factor of 30 *smaller* than the value given above, the space constant for current flow through this frustrum is about 100 μ; significantly *greater* than the thickness of the frustrum plus cell (51 μ). In this calculation we assumed that the internal resistivity was 100 Ω cm and that the average radius was 0.85 μ. The maximum error, therefore, is 17% and 6000–7000 Ω cm^2 remains a good estimate of R_a.

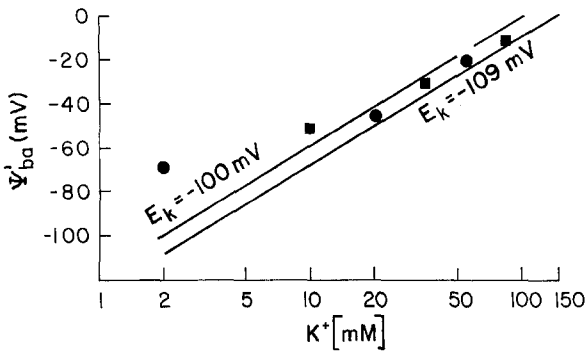

Fig. 12. Ψ'_{ba} as a function of *basal* $[K^+]$. The filled circles and squares above 2 mM are calculated from the value of Ψ'_{ba} at 2 mM and the data of Fig. 11. The solid lines are the Nernst lines for $E_K = -100$ and -109 mV

the size of Δa, for changes from 2 to 20 and 55 mM (Table 2). Therefore, the data of Fig. 11 and the value of Ψ'_{ba} have been used in Fig. 12 to estimate intracellular $[K^+]$. The data lie between the two Nernst lines for $E_K = -100$ mV and $E_K = -109$ mV. These equilibrium potentials correspond, respectively, to $[K^+]_i = 110$ mM and $[K^+]_i = 150$ mM. There are reasons for accepting $E_K = -100$ mV as the more correct value for determing intracellular $[K^+]$. When basal $[K^+]_o$ is raised from $2 \rightarrow 55$ mM, for example, any elevation of $[K^+]_i$ or even a small Na^+ diffusion potential would tend to reduce the size of the $\Delta\Psi'_{ba}$ response; therefore, the data plotted in Fig. 12 would rise toward the $E_K = -100$ mV line. More importantly, in the fast perfusion experiments ($2 \rightarrow 55$ mM K^+), 15–18 cc/min, the voltage response is much faster and within 1 min its size is about what one would expect of a K^+ electrode with $E_K = -100$ mV.

This work was supported by National Eye Institute Research grants EY-00468 (to Kenneth T. Brown) and EY-01429 to (R.S.); by Career Development Award EY-18073 (to R.S.), by Postdoctoral Research Fellowship EY-49436 (to S.M.) and by a Fight for Sight Grant (G-525, to S.M.). We thank Warren S. Rehm for helping us to clarify the theoretical section. We wish to thank Paula L. Lacy, Steven Dong, Yu Hwong and Herman Chibnik for technical assistance; and also Juan Korenbrot and Michael F. Marmor for their comments on an earlier version of this manuscript.

Appendix

To estimate the error of using Eq. (10) when a is not constant we start with the more general Eq. (25a) and rewrite it in the form of Eq. (10) plus

an error term. That is,

$$a\Psi_{ap}^{*}-a^{*}\Psi_{ap}+aa^{*}\Delta\Psi_{ba}=a\Psi_{ap}'^{*}-a^{*}\Psi_{ap}'. \tag{A.1}$$

Let $a^{*}\equiv Ka$ where $K>1$ for all increases in $[K^{+}]_o$ relative to 2 mM and decreases in $[HCO_3^{-}]_o$ relative to 27.5 mM. Replacing a^{*} by Ka and $\Delta\Psi_{ba}$ by $\Delta\Psi_{ap}-\Delta\mathrm{TEP}$ we obtain

$$a\Psi_{ap}^{*}-Ka\Psi_{ap}+Ka^{2}(\Delta\Psi_{ap}-\Delta\mathrm{TEP})=a\Psi_{ap}'^{*}-Ka\Psi_{ap}' \tag{A.2}$$

which can be rewritten as

$$\Delta\Psi_{ap}-(K-1)\Psi_{ap}+Ka(\Delta\Psi_{ap}-\Delta\mathrm{TEP})=\Delta\Psi_{ap}'-(K-1)\Psi_{ap}'.$$

After a little algebra we obtain

$$\Delta\Psi_{ap}'+(1+a)\Delta\Psi_{ap}-a\Delta\mathrm{TEP}+|E_r| \tag{A.3}$$

where

$$|E_r|=(K-1)[a|\Delta\Psi_{ba}|-|\Psi_{ap}-\Psi_{ap}'|].$$

The two terms in the brackets are of opposite sign regardless of the sign convention for intracellular potentials; therefore, absolute values are used. From Eqs. (1) and (3a) the above expression is rewritten as

$$|E_r|=\left(\frac{a^{*}}{a}-1\right)\left[a|\Delta\Psi_{ba}|-\frac{|\mathrm{TEP}|}{\left(1+\frac{1}{a}\right)[(R_s/R_t)-1]}\right].$$

Except for R_s, all the quantities in this expression are known. Once a value for R_s is assumed $|E_r|$ is determined and R_a and R_b can be calculated from Eq. (1).

For example, for one of the cells summarized in Table 1, $a=0.5$, $a^{*}=0.83$, TEP = 8.8 mV, $R_t=3500\,\Omega$ and $\Delta\Psi_{ba}=6$ mV. Therefore,

$$|E_r|=2\,\mathrm{mV}-\frac{1.9\,\mathrm{mV}}{(R_s/R_t)-1}.$$

If $R_s/R_t=2$ is substituted into the above expression and into Eq. (1) one obtains

$$|E_r|=0.1\,\mathrm{mV},\quad R_a=2333\,\Omega,\quad R_b=4666\,\Omega,\quad R_s=7000\,\Omega.$$

These calculated quantities and the recorded membrane potential changes are used in Eqs. (25) to calculate the "correct" value of $\Delta\Psi_{ap}'$. We have demonstrated in Fig. 5 that part of the potential change at one

membrane is shunted to the opposite side and therefore $\Delta\Psi'_{ap} > \Delta\Psi_{ap}$. This constraint allows us to put a lower bound on the value of R_s. In the above example, $\Psi_{ap} = -99\,\text{mV}$ and from Eq. (27b) $\Psi'_{ap} = -101.9\,\text{mV}$ while from Eqs. (25) $\Delta\Psi'_{ap} = 14\,\text{mV}$. The constraint $\Delta\Psi'_{ap} > \Delta\Psi_{ap}$ (11 mV) is therefore satisfied and the assumption $R_s/R_t = 2$ cannot be rejected. If, however, $R_s/R_t = 1.25$ then $\Delta\Psi'_{ap} \approx 8\,\text{mV} < \Delta\Psi_{ap}$. Since the constraint is violated, R_s/R_t must be greater than 1.25. In fact, the smallest possible value of R_s/R_t for which the constraint is not violated is 1.4. In this case $R_s = 4900\,\Omega$ and $|E_r| = 2.7\,\text{mV}$.

In general, if we choose a value of R_s such that the above constraint is violated then all values of R_s smaller than the chosen one will also violate. On the other hand, if we pick a value of R_s such that the inequality is satisfied, all values of R_s greater than the chosen value will also satisfy. This explains the direction of the inequality in column 9, Table 1. Column 8 in these Tables contains the calculated maximum theoretical error in assuming a constant. In most cases the error is obtained by letting $R_s \to \infty$. This assumption is clearly contradicted by the data in Fig. 5 and by the calculated values of R_s shown in Table 2. Therefore, the actual error is probably a factor of 2 or 3 smaller than the values in column 8.

References

Aickin, C.C., Thomas, R.C. 1975. Micro-electrode measurement of the internal pH of crab muscle fibers. *J. Physiol. (London)* **252**:803

Barry, P.H., Diamond, J.H. 1970. Junction potentials, electrode standard potentials, and other problems in interpreting electrical properties of membranes. *J. Membrane Biol.* **3**:93

Boulpaep, E.L. 1967. Ion permeability of the peritubular and luminal membrane of the renal tubular cell. *In:* Transport und Funktion intracellulärer Elektrolyte. F. Kruck, editor. p. 98. Urban and Schwarzenberg, München

Boulpaep, E.L. 1971. Electrophysiological properties of the proximal tubule: Importance of cellular and intercellular pathways. *In:* Electrophysiology of Epithelia. G. Giebisch, editor. p. 91. K. Schattauer Verlag, Stuttgart

Brown, K.T., Flaming, D.G. 1974. Beveling of fine micropipette electrodes by a rapid precision method. *Science* **185**:693

Casteels, R., Droogman, G., Hendrickx, H. 1971. Membrane potential of smooth muscle cells in *K*-free solution. *J. Physiol. (London)* **217**:281

Diamond, J. 1966. A rapid method for determining voltage-concentration relations across membranes. *J. Physiol. (London)* **183**:83

Dowling, J.E. 1960. Chemistry of visual adaptation in the rat. *Nature (London)* **188**:114

Finkelstein, A., Mauro, A. 1963. Equivalent circuits as related to ionic systems. *Biophys. J.* **3**:215

Frömter, E. 1972. The route of passive ion movement through the epithelium of *Necturus* gallbladder. *J. Membrane Biol.* **8**:259

Frömter, E., Diamond, J. 1972. Route of passive ion permeation in epithelia. *Nature New Biol.* **235**:9

Hagiwara, S., Fukuda, J., Eaton, D.C. 1974. Membrane currents carried by Ca, Sr and Ba in barnacle muscle fiber during voltage clamp. *J. Gen. Physiol.* **63**:564

Helman, S.I., Miller, D.A. 1973. Edge damage effect on electrical measurements of frog skin. *Am. J. Physiol.* **225**:972

Hodgkin, A.L., Horowicz, P. 1959. The influence of potassium and chloride ions on the membrane potential of single muscle fibers. *J. Physiol. (London)* **148**:127

Hudspeth, J.A., Yee, A.G. 1973. The intercellular junctional complexes of retinal pigment epithelia. *Invest. Ophthalmol.* **12**:354

Kidder, G.W., III, Cereijido, M., Curran, P.F. 1964. Transient changes in electrical potential difference across frog skin. *Am. J. Physiol.* **207**:935

Kostyuk, P.G., Krishtal, O.H., Pidoplichko, V.I. 1972. Potential-dependent membrane current during the active transport of ions in snail neurons. *J. Physiol. (London)* **226**:373

Kuwabara, T. Species differences of the pigment epithelium. *In:* The Retinal Pigment Epithelium. K.M. Zinn and M.F. Marmor, editors. Harvard University Press, Cambridge *(in press)*

Lasansky, A., DeFisch, F.W. 1966. Potential, current and ionic fluxes across the isolated retinal pigment epithelium and choroid. *J. Gen. Physiol.* **49**:913

MacInnes, D.A. 1961. The Principles of Electrochemistry, 2nd ed. Dover Publications, New York, p. 52

Miller, S.S., Steinberg, R.H. 1977. Active transport of ions across frog retinal pigment epithelium. *Exp. Eye Res. (in press)*

Nilsson, S.E.G. 1964. An electron microscopic classification of the retinal receptors of the leopard frog (*Rana pipiens*). *J. Ultrastruct. Res.* **10**:390

Noell, W.K., Crapper, D.R., Paganelli, C.V. 1965. Transretinal currents and ion fluxes. *In:* Transcellular Membrane Potentials and Ionic Fluxes. F. Snell and W.K. Noell, editors. Gordon and Breach, New York

Paillard, M. 1972. Direct intracellular pH measurement in rat and crab muscle. *J. Physiol. (London)* **223**:297

Porter, K.R., Yamada, E. 1960. Studies on the endoplasmic reticulum. V. Its form and differentiation in pigment epithelial cells of the frog retina. *J. Biophys. Biochem. Cytol.* **8**:181

Reuss, L., Finn, A.L. 1974. Passive electrical properties of toad urinary bladder epithelium. Intercellular electrical coupling and transepithelial cellular and shunt conductances. *J. Gen. Physiol.* **64**:1

Rose, R.C., Schultz, S.G. 1971. Studies on the electrical potential profile across rabbit ileum. Effects of sugars and amino acids on transmural and transmucosal P.D.'s. *J. Gen. Physiol.* **57**:639

Rothe, C.F., Quay, J.F., Armstrong, W.F. 1969. Measurement of epithelial electrical characteristics with an automatic voltage clamp device with compensation for solution resistance. *IEEE Trans. Bio-Med. Engrg.* **BME-16 (No. 2)**:160

Schultz, S.G. 1974. Principles of electrophysiology and their application to epithelial tissues. *In:* Gastrointestinal Physiology. E.D. Jacobson and L.S. Shanbur, editors. Vol. 4, p. 69. University Park Press, Baltimore

Spangler, S.G., Rehm, W.S. 1968. Potential responses of nutrient membrane of frog's stomach to step changes in external K^+ and Cl^- concentrations. *Biophys. J.* **8**:1211

Spenny, J.G., Flemstrom, G., Shoemaker, R.L., Sachs, G. 1975. Quantitation of conductance pathways in antral gastric mucosa. *J. Gen. Physiol.* **65**:645

Spenny, J.G., Shoemaker, R.L., Sachs, G. 1974. Microelectrode studies of fundic gastric mucosa: Cellular coupling and shunt conductance. *J. Membrane Biol.* **19**:105

Steinberg, R.H. 1973. Scanning electron microscopy of the bullfrog's retina and pigment epithelium. *Z. Zellforsch.* **143**:451

Steinberg, R.H., Miller, S. 1973. Aspects of electrolyte transport in frog pigment epithelium. *Exp. Eye Res.* **16**:365

Thomas, R.C. 1974. Intracellular pH of snail neurones measured with a new pH-sensitive glass microelectrode. *J. Physiol. (London)* **238**:159

Woodbury, J.W. 1971. Fluxes of H^+ and HCO_3^- across frog skeletal muscle cell membranes. *In:* Ion Homeostasis of the Brain. B.K. Siesjo and S.C. Sorenson, editor. p. 270. Munksgaard, Copenhagen

Wright, E.M., Diamond, J.M. 1968. Effects of pH and polyvalent cations on the selective permeability of gall-bladder epithelium to monovalent ions. *Biochim. Biophys. Acta* **163**:57

Young, R.W. 1969. The organization of vertebrate photoreceptor cells. *In:* The Retina. B.R. Straatsma, M.O. Hall, R.A. Allen, and F. Crescitelli, editors. p. 177. University of California Press, Berkeley and Los Angeles